Effect of Torrefaction on Biomass Structure and Product Distribution from Fast Pyrolysis

by

Sneha Neupane

A thesis submitted to the Graduate Faculty of
Auburn University
in partial fulfillment of the
requirements for the Degree of
Master of Science

Auburn, Alabama
May 9, 2015

Keywords: biomass, torrefaction, pyrolysis, characterization, catalyst

Approved by

Sushil Adhikari, Chair, Associate Professor of Biosystems Engineering
Oladiran Fasina, Professor of Biosystems Engineering
Maobing Tu, Associate Professor of Forestry and Wildlife Sciences
Peng Zeng, Associate Professor of Statistics

Abstract

Torrefaction, a thermal pretreatment process, has been documented to improve the chemical composition of bio-oil produced from fast pyrolysis process. During torrefaction pretreatment, the major constituents of biomass (cellulose; hemicellulose and lignin) undergo various structural and chemical changes that can affect the reaction pathways during fast pyrolysis process and favor the production of certain compounds. The main focus of this study was to understand biomass torrefaction chemistry and determine how it subsequently affects the product distribution from non-catalytic and H^{+}ZSM-5 catalyzed fast pyrolysis. Samples were torrefied at three temperatures (225, 250 and 275 ^{o}C) and for three residence times (15, 30 and 45 min), for a total of nine treatments. Loblolly pinewood was used for the study due to its abundant availability in the southeast United States.

The structural transformations in the biomass constitutive polymers were evaluated using component analysis, solid state CP/MAS ^{13}C NMR and XRD techniques. Component analysis was carried out to quantify the weight percentage of cellulose, hemicellulose and lignin degradation at different torrefaction severity while, XRD and ^{13}C NMR were used to quantify biomass structural changes like cellulose crystallinities and fractions of carbonyl, aromatic, alkyl, ether and methoxyl carbons in torrefied samples. Torrefaction caused degradation (starting at 225^{o}C-30min) and deacetylation (starting at 225^{o}C-15min) of hemicellulose components. Initial wt. loss of 23% in lignin was observed at 225^{o}C-30min due to de-methoxylation and de-

etherification of lignin. Cellulose degradation occurred at higher torrefaction severity (225^{o}C - 45min, 250^{o}C - 30 and 45 min, and 275^{o}C -15, 30 and 45 min) and was accompanied by overall increase in aromaticity of biomass.

Py-GC/MS study was carried out to study the chemical composition of pyrolyic vapor from raw and torrefied samples. For non-catalytic pyrolysis, selectivity of aromatic hydrocarbon (HC) and phenolic compounds increased with increase in torrefaction severity while that of furan compounds decreased. These were attributed to increase in aromaticity of biomass, changes in structure of lignin and degradation of hemicellulose, respectively. In case of catalytic pyrolysis, the samples torrefied at 225^{o}C-30min and 250^{o}C-15min resulted in significant increase in aromatic HC and also total carbon yield (approx. 1.6 times higher) as compared to catalytic pyrolysis of raw pine. De-etherification and de-methoxylation of lignin occurred at these torrefaction conditions causing increased yield of phenolic compounds, which in presence of catalyst were dehydrated to form aromatic HC. Aromatic HC yield from catatytic pyrolysis was also found to be directly proportional to wt.% of cellulose and inversely to aromaticity of torrefied biomass.

Acknowledgements

My deepest appreciation goes to my advisor Dr. Sushil Adhikari. His encouragement, enthusiasm and faith in me have been extremely helpful throughout, and I have gained much insight from his knowledge in this field. I also thank my committee members: Dr. Maobing Tu, Dr. Oladiran Fasina, and Dr. Peng Zeng. I am also grateful to our post-doctoral researcher Dr. Zhouhong Wang for helping me with experiments and providing valuable suggestions and comments that have led to improvement of this work. I am thankful to Vaishnavi for training me to operate GC/MS, and Nour for helping me with XRD analysis. Special thanks to Dr. Arthur J. Ragauskas of Paper Science Institute at Georgia Tech. for carrying out NMR experiments and providing valuable feedback on the Chapter 3. I also want to thank my family and friends for their continuous encouragement and support. Lastly, I would like to acknowledge the funding agency that made this research possible. This work was supported by the Energy for Sustainability of National Science Foundation (Award Number: 1333372).

Table of Contents

Abstract ii

Acknowledgements iv

Table of Contents v

List of Figures viii

List of Tables ix

1. Introduction 1

1.1. Objectives 2

1.1.1. Investigate the effect of torrefaction on biomass structure 3

1.1.2. Understand the effect of biomass structure on product distribution from fast pyrolysis 3

1.2. References 4

2. Literature Review 6

2.1. Structure of lignocellulosic biomass 7

2.2. Torrefaction 11

2.2.1. Introduction 11

2.2.2. Characteristics of torrefied biomass 12

2.2.3. Reactions and mechanisms 13

2.2.4. Factors affecting torrefaction 15

2.3. Fast pyrolysis 16

2.4. Bio-oil characteristics 18

2.5. Fast pyrolysis chemistry and product distribution 19

2.6. Catalytic fast pyrolysis 22
2.7. Fast pyrolysis of biomass pretreated by torrefaction 23
2.8. References 25
3. Effect of Torrefaction on Biomass Structure and Hydrocarbons Production from Fast Pyrolysis 34
3.1. Abstract 34
3.2. Introduction 35
3.3. Material and Methods 37
3.3.1. Material and sample preparation 37
3.3.2. Component analysis 39
3.3.3. CP MAS ^{13}C NMR 40
3.3.4. XRD 41
3.3.5. Py-GCMS 41
3.4. Results 43
3.4.1. Component analysis 43
3.4.2. CP MAS ^{13}C NMR 44
3.4.3. XRD 53
3.4.4. Py-GC/MS: Non-catalytic pyrolysis 55
3.4.5. Py-GC/MS: Catalytic pyrolysis 60
3.5. Discussion 63
3.6. Conclusions 72
3.7. References 73
4. Summary and Future Recommendations 78
4.1. Summary 78
4.2. Recommendations 79
APPENDIX A: Component and ^{13}C NMR analyses 81

APPENDIX B: Data for graphs 83

List of Figures

Figure 2.1 Structure of the main components of wood (a) cellulose (b) xylan (main component of hemicelluloses) (c) building blocks lignin 10

Figure 2.2 Different linkages in lignin (a) β-O-4 (b) 4-O-5 (c) β-β (d) β-5 (e) 5-5 11

Figure 2.3 Bio-oil compounds and their relative abundance 21

Figure 3.1 ^{13}C NMR Spectra of (from top to bottom): Control, 225^{o}C-15min, 225^{o}C-30min, 225^{o}C-45min, 225^{o}C-15min, 250^{o}C-30min, 250^{o}C-45min, 275^{o}C-15min, 275^{o}C-30min, 275^{o}C-45min 46

Figure 3.2 Normalized area of hemicellulose components at different torrefaction conditions a) Acetyl carboxyl b) Acetyl methyl 48

Figure 3.3 Normalized area of total glyosidic linkages at different torrefaction conditions 49

Figure 3.4 Normalized area of lignin components at different torrefaction conditions a) Ether linked b) Non-ether linked c) Lignin methoxyl 51

Figure 3.5 Normalized areas of a) Aromatic and b) Aliphatic signals at different torrefaction condition 53

Figure 3.6 XRD spectra (from bottom to top): Control, 225^{o}C-15min, 225^{o}C-30min, 225^{o}C-45min, 225^{o}C-15min, 250^{o}C-30min, 250^{o}C-45min, 275^{o}C-15min, 275^{o}C-30min, 275^{o}C-45min 54

Figure 3.7 Selectivity of different compounds with torrefaction severity for non-catalytic pyrolysis 60

Figure 3.8 Plot of aromatic HC yield from non-catalytic pyrolysis versus aromatic components in biomass 65

Figure 3.9 Yield of furan compounds versus wt.% of hemicellulose in biomass 66

Figure 3.10 Predicted phenolic yield versus actual phenolic yield 67

Figure 3.11 Plot of aromatic HC yield from catalytic pyrolysis vs a) wt.% of cellulose and b) aromatic components in biomass 70

List of Tables

Table 2.1 Fraction of cellulose, hemicellulose and lignin in lignocellulosic biomass 11

Table 3.1 Nomenclature used for samples torrefied at different conditions..... 38

Table 3.2 Physical and chemical properties of torrefied loblolly pine (dry basis) 39

Table 3.3 Component analysis (wt.%)..... 44

Table 3.4 Assignment of signal from CP/MAS ^{13}C NMR 45

Table 3.5 CrI of control and torrefied samples..... 55

Table 3.6 List of compounds quantified for non-catalytic pyrolysis..... 56

Table 3.7 Carbon yield % from non-catalytic pyrolysis..... 56

Table 3.8 List of compounds quantified for catalytic pyrolysis 62

Table 3.9 Carbon yield% from catalytic fast pyrolysis of raw and torrefied samples..... 63

Table 3.10 Overall summary of effect of torrefaction on biomass components (as compared to control sample)..... 64

Table 3.11 Product yield from catalytic and non-catalytic pyrolysis accounting for carbon loss during torrefaction 72

Table A.1 Results of component analysis, wt. %, dry basis (Not normalized by mass loss) 81

Table A.2 ^{13}C NMR Area (Not normalized by mass loss) 82

Table B.1 ^{13}C NMR normalized area (Data for Figures 3.2 – 3.5)..... 83

Table B.2 Selectivity of different groups of compounds for non-catalytic pyrolysis (Data for Figure 3.7)..... 83

1. Introduction

The United States currently imports over nine million barrels of oil per day (as of August 2014) [1], cost of which is likely to increase in future due to increasing global demand and depleting oil reserves. The world oil reserve is predicted to be sufficient to meet the projected growth in demand until 2030 [2], with the organization of petroleum exporting countries (OPEC) more likely to continue to dominate the market and control the prices [3]. In addition to this, increased concerns over greenhouse gas (GHG) emissions have intensified the search for renewable and more affordable domestic alternatives to imported petroleum oil. The United States Energy Independence and Security Act (EISA) of 2007 has mandated production of 36 billion gallons of renewable transportation fuels (sufficient to replace 20% of the crude oil demand) by 2022, of which 21 billion gallons must be "advanced biofuels" that are derived from lignocellulosic biomass feedstock [4]. Production of renewable fuels from lignocellulosic biomass has the advantage of abundant availability of raw material like logging residues, small diameter trees, agricultural residues and wastes and dedicated energy crops that can be used to produce biofuel without threatening food supplies. However, due to complex nature of lignocellulosic biomass, several steps are required to convert it into fuels.

One of the ways to convert biomass to liquid fuels is via fast pyrolysis process. In fast pyrolysis process, vapors formed from rapid heating of biomass are quickly condensed to produce liquid fuel, known as bio-oil, which can be used in variety of applications and as energy carrier [5]. However, bio-oil is acidic, unstable and has low heating value and high oxygen content. These

characteristics restrict their use as a conventional transportation fuel [6]. Catalytic fast pyrolysis of biomass using zeolite catalyst is a promising way to improve the quality of bio-oil in terms of chemical composition. During catalytic fast pyrolysis, compounds in pyrolytic vapor are deoxygenated to produce stable bio-oil that is rich in aromatic hydrocarbons in a single step [7-9]. The major problem with catalytic fast pyrolysis is formation of undesired coke, which results in decreased yield of liquid product [7, 10, 11].

The focus of this thesis was to study the effect of torrefaction pretreatment on product distribution from fast pyrolysis process (non-catalytic and catalytic). Torrefaction is thermal treatment of biomass in temperature range 200-300 ^{o}C, mainly targeted to enhance heating value of biomass. It has already shown some promising results for energy production: co-firing with coal and producing energy dense pellets [12, 13]. Recently, it has been tested for producing bio-oil as well [14-20]. Studies have reported improvement in quality (i.e. chemical composition) of bio-oil produced from torrefied biomass as compared to untreated biomass. Torrefaction pretreatment is also reported to increase hydrocarbons yields from catalytic fast pyrolysis using zeolite catalysts [14, 21]. The hypothesis of this study is that torrefaction pretreatment can alter the structure of biomass building blocks (cellulose hemicellulose and lignin) and change the reaction pathway during fast pyrolysis favoring the formation of certain bio-oil compounds.

1.1. Objectives

The objective of this study was to understand biomass torrefaction chemistry, and its impact on non-catalytic and catalytic pyrolysis for hydrocarbons production. This overall objective was accomplished by two specific objectives listed below.

1.1.1. Investigate the effect of torrefaction on biomass structure

The structural transformations in the biomass constitutive polymers: cellulose, hemicellulose and lignin were evaluated using component analysis, solid state CP/MAS (cross polarization/ mass angle spinning) ^{13}C NMR (Carbon-13 Nuclear Magnetic Resonance) and XRD (X-ray diffraction) techniques. Component analysis was carried out to quantify the weight % (wt.%) of cellulose, hemicellulose and lignin degradation at different torrefaction severity. XRD and ^{13}C NMR were used quantify structural changes like cellulose crystallinities and fractions of acetyl, aromatic, alkyl, ether and methoxyl carbon in torrefied samples.

1.1.2. Understand the effect of biomass structure on product distribution from fast pyrolysis

Pyrolysis of biomass torrefied at different severity was carried out with and without catalyst (H^+ZSM-5) using a commercial pyroprobe, and the pyrolytic vapors were analyzed using gas chromatograph coupled with mass spectrometer (GC/MS). For all experiments, pyrolysis temperature and heating rate were fixed at 550 ^oC and 2000 ^oC/sec, respectively. Biomass to catalyst ratio of 1:9 was used for catalytic pyrolysis experiments. Relationship between biomass structure and product yield from fast pyrolysis were established using multiple linear regression and biomass properties that are important in aromatic production were quantified.

1.2. References

1. *Energy Information Administration, 2014. US imports by country of origin, August 2014. Available at http://www.eia.gov/dnav/pet/pet_move_impcus_a2_nus_ep00_im0_mbbl_m.htm.*

2. Chedid, R., M. Kobrosly, and R. Ghajar, *A supply model for crude oil and natural gas in the Middle East.* Energy policy, 2007. **35**(4): p. 2096-2109.

3. Shafiee, S. and E. Topal, *When will fossil fuel reserves be diminished?* Energy Policy, 2009. **37**(1): p. 181-189.

4. *Public Law 110–140, 2007. Energy Independence and Security Act of 2007, Available at http://leahy.senate.gov/issues/FuelPrices/EnergyIndependenceAct.pdf.*

5. Bridgwater, A., *Principles and practice of biomass fast pyrolysis processes for liquids.* Journal of Analytical and Applied Pyrolysis, 1999. **51**(1): p. 3-22.

6. Czernik, S. and A. Bridgwater, *Overview of applications of biomass fast pyrolysis oil.* Energy & Fuels, 2004. **18**(2): p. 590-598.

7. Carlson, T.R., T.P. Vispute, and G.W. Huber, *Green gasoline by catalytic fast pyrolysis of solid biomass derived compounds.* ChemSusChem, 2008. **1**(5): p. 397-400.

8. Carlson, T.R., et al., *Production of green aromatics and olefins by catalytic fast pyrolysis of wood sawdust.* Energy & Environmental Science, 2011. **4**(1): p. 145-161.

9. Carlson, T.R., et al., *Catalytic fast pyrolysis of glucose with HZSM-5: the combined homogeneous and heterogeneous reactions.* Journal of Catalysis, 2010. **270**(1): p. 110-124.

10. Gayubo, A.G., et al., *Transformation of oxygenate components of biomass pyrolysis oil on a HZSM-5 zeolite. I. Alcohols and phenols.* Industrial & Engineering Chemistry Research, 2004. **43**(11): p. 2610-2618.

11. Gayubo, A.G., et al., *Transformation of oxygenate components of biomass pyrolysis oil on a HZSM-5 zeolite. II. Aldehydes, ketones, and acids.* Industrial & Engineering Chemistry Research, 2004. **43**(11): p. 2619-2626.

12. Van der Stelt, M., et al., *Biomass upgrading by torrefaction for the production of biofuels: a review.* Biomass and Bioenergy, 2011. **35**(9): p. 3748-3762.

13. Pimchuai, A., A. Dutta, and P. Basu, *Torrefaction of agriculture residue to enhance combustible properties.* Energy & Fuels, 2010. **24**(9): p. 4638-4645.

14. Srinivasan, V., et al., *Catalytic pyrolysis of torrefied biomass for hydrocarbons production.* Energy & Fuels, 2012. **26**(12): p. 7347-7353.

15. Liaw, S.-S., et al., *Effect of pretreatment temperature on the yield and properties of bio-oils obtained from the auger pyrolysis of Douglas fir wood.* Fuel, 2013. **103**: p. 672-682.

16. Meng, J., et al., *The effect of torrefaction on the chemistry of fast-pyrolysis bio-oil.* Bioresource Technology, 2012. **111**(0): p. 439-446.

17. Zheng, A., et al., *Effect of torrefaction temperature on product distribution from two-staged pyrolysis of biomass.* Energy & Fuels, 2012. **26**(5): p. 2968-2974.

18. Zheng, A., et al., *Effect of torrefaction on structure and fast pyrolysis behavior of corncobs.* Bioresource Technology, 2013. **128**(0): p. 370-377.

19. Hilten, R.N., et al., *Effect of torrefaction on bio-oil upgrading over HZSM-5. Part 1: Product yield, product quality, and catalyst effectiveness for benzene, toluene, ethylbenzene, and xylene production.* Energy & Fuels, 2013. **27**(2): p. 830-843.

20. Hilten, R.N., et al., *Effect of torrefaction on bio-oil upgrading over HZSM-5. Part 2: Byproduct formation and catalyst properties and function.* Energy & Fuels, 2012. **27**(2): p. 844-856.

21. Adhikari, S., V. Srinivasan, and O. Fasina, *Catalytic pyrolysis of raw and thermally treated lignin using different acidic zeolites.* Energy & Fuels, 2014. **28**(7): p. 4532–4538.

2. Literature Review

Lignocellulosic biomass can be converted to more valuable forms of energy via a number of processes including thermal, biological, mechanical or physical processes. Biological conversion involves biochemical processing of biomass into valuable fuels using biological catalyst (microorganisms) and the process takes relatively longer time (2 to 5 days) to complete. Thermal conversion process use heat and inorganic catalyst and take place in very short reaction time (0.2 sec. to 1 hr.). Biological processing results in high yield of discrete products (such as ethanol) while thermal processing often results in multiple and complex products [1].

The three main thermal processes for conversion of biomass resources to fuels and chemicals are combustion, gasification and pyrolysis. Combustion is a well-established commercial technology in which biomass is burned in air to generate heat. In gasification process, solid carbonaceous material is converted into a mixture of combustible gases known as syngas, by partial combustion process, which can be directly used for heat or power, and also synthesized into liquid fuels. Gasification is usually carried out at temperatures above 600 ^{o}C [1]. Pyrolysis involves heating of biomass (400-600 ^{o}C) in absence of oxygen to produce char, vapors, aerosols and gases. Vapors and aerosols can be condensed to form liquid fuel called bio-oil. Slow heating rates of 5 to 10 ^{o}C/min during pyrolysis results in enhanced char production and reduced liquid yield, and therefore typically used to produce charcoal. [2]. In fast pyrolysis process high heating rate (>500 ^{o}C/s) is used to produce mostly vapors and aerosols, which after rapid cooling (vapor residence time = 1-2 sec) condense to form bio-oil [3]. Low temperature pyrolysis (200 – 300

^{o}C) process called torrefaction is also recently gaining attention as an important pre-processing step to enhance the fuel properties of biomass. This study is mainly focused on use of torrefaction for biomass pretreatment prior to fast pyrolysis process, in order to improve the chemical composition of final liquid fuel (bio-oil). Structure of lignocellulosic biomass, torrefaction and fast pyrolysis processes are discussed in details in upcoming sections.

2.1. Structure of lignocellulosic biomass

Lignocellulosic biomass is composed mainly of cellulose, hemicellulose, and lignin and smaller amounts of ash and extractives. The crystalline cellulose fibrils is bound by non-crystalline hemicellulose and surrounded by a matrix of hemicellulose and lignin [4, 5] to form a complex and rigid structure of lignocellulosic biomass. The extractives in biomass include oils, gums, waxes, pectin, and proteins [6]. Ash is mineral that consists of alkali and alkaline earth metals and all other non-combustible components of biomass. Lignocellulosic biomass can be directly or indirectly used for the production of biomolecules and commodity chemicals through different types of biochemical and thermochemical processings [7, 8]. However, the complex structure and close association among the three constitutive polymers limit the conversion processes and applications in variety of ways. Therefore, a clear understanding of biomass chemistry is necessary to achieve the optimum conversion of these polymers into valuable fuels and chemicals.

Cellulose is the most abundant organic material on earth with molecular formula of $C_6H_{10}O_5$. It is composed of a linear chain of D-glucose units linked with glycosidic bond (β 1-4 linkage) as shown in Figure 2.1(a) [9]. The degree of polymerization of cellulose is in the range of 7000 –

15000. These chains are arranged in parallel direction connected by intramolecular hydrogen bonds between adjacent chains to form highly compact crystalline molecular structure of microfibrils. Microfibrils impart strength to the plant structure and cell walls. Non-crystalline and less ordered region within the microfibril structure is referred to as amorphous cellulose [10, 11]. Many studies in the past have shown that amorphous areas can be more easily broken down by hydrolysis compared to crystalline regions [12-14]. The glycosidic linkages of cellulose are hydrolyzed in the presence of enzymes to release glucose, which can be fermented to produce ethanol or butanol. Such biochemical conversion process occurs at low temperature and takes longer time (2 - 5 days) to complete [1]. On the other hand, thermochemical processes, which occur at very high temperature and short reaction time rapidly depolymerize cellulose to produce primarily levoglucosan – an anhydrosugar of glucose [15].

Hemicellulose is a highly branched structure, primarily composed of short chains of hetero-1, 4-β-D-xylan [16]. The degree of polymerization is 70 – 200. Hemicellulose is amorphous and hydrophilic; therefore, it can be easily hydrolyzed by chemical treatments and enzymatic hydrolysis and is also more vulnerable to thermochemical pretreatment. The major hemicelluloses in softwoods are galactoglucomannans and arabinoglucuronoxylan, while the predominant hemicellulose in hardwoods is glucuronoxylan.

Lignin, after cellulose is the second most abundant bio-polymeric organic natural product on earth. It is an amorphous, cross-linked phenolic macromolecule with relatively high molecular masses [17]. It is composed of three different primary hydroxycinnamyl alcohols that are p-coumaryl, conifer, and sinapyl alcohol. The corresponding phenylpropanoid monomers are usually denoted as p-hydroxyphenyl (H), guaiacyl (G), and syringyl (S) units, respectively, based on methoxy substitution on the aromatic rings as shown in Figure 2.1(c). In general, softwood

lignin is mainly composed of G units with small quantity of H units (G/S/H = 96:t:4), and hardwood lignin consists of similar levels of G and S units with traces of H units (G/S/H = 50:50:t). Grasses lignin consists of all three units in the ratio of G/S/H = 70:25:5 [18]. The three lignin monomers are interconnected with different type of linkages: β-O-4, 4-O-5, β-β, β-5 and 5-5 (Figure 2.2), the relative abundance of which depend largely on relative contribution of monomer to the polymerization process during lignin biosynthesis. The β-O-4 (aryl glycerol-β-aryl ether) linkage shown in Figure 2.2(a) creates most abundant structure, generally involving 50% and 60% of phenylpropanoid units in softwood and hardwood lignin respectively [19]. Chemical bonds have been reported between lignin and carbohydrates (hemicellulose and cellulose) to form covalently bonded lignin-carbohydrate complex (LCC). The linkages are formed by ester, ether and glycosidic types of bonds [20]. Lignin has been considered as a physical barrier during biochemical conversion process as it protects the carbohydrate from biological attack [1]. As lignin constitutes around 25 wt.% of lignocellulosic biomass, improving its utilization can enhance the overall lignocellulosic bio-refinery [1]. Thermochemical conversion process like fast pyrolysis can depolymerize lignin to form phenolic compounds [21]. The relative abundance of these three components in softwood, hardwood and grass is shown in Table 2.1.

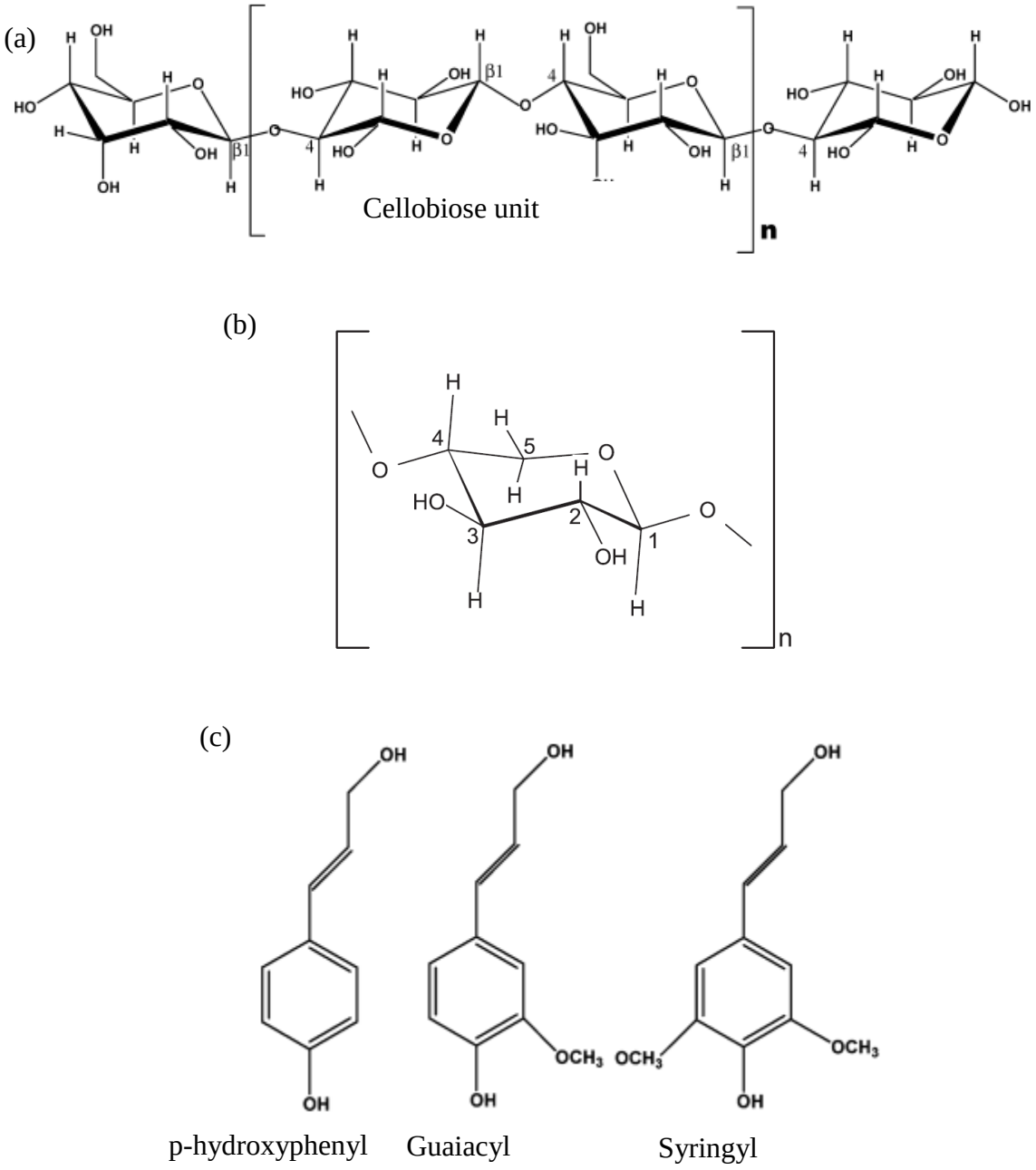

Figure 2.1 Structure of the main components of wood (a) cellulose [22] (b) xylan (main component of hemicelluloses) [23] (c) building blocks lignin [22]

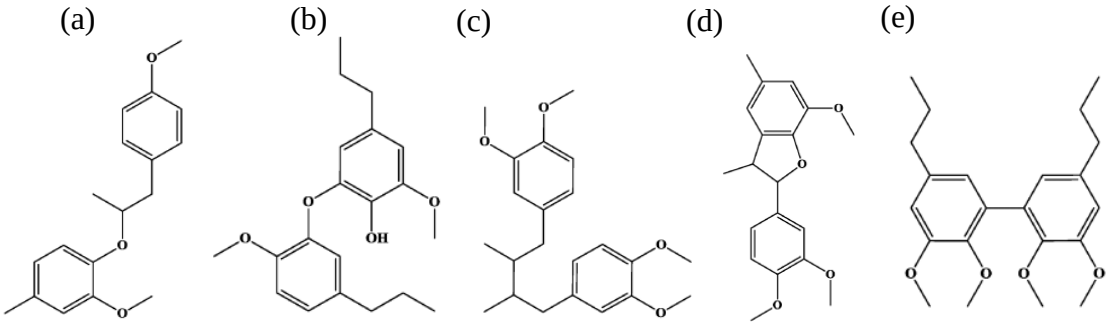

Figure 2.2 Different linkages in lignin [24] (a) β-O-4 (b) 4-O-5 (c) β-β (d) β-5 (e) 5-5

Table 2.1 Fraction of cellulose, hemicellulose and lignin in lignocellulosic biomass [25]

Biomass	Lignin (%)	Cellulose (%)	Hemi-cellulose (%)
Softwood	27-30	35-40	25-30
Hardwood	20-25	45-50	20-25
Wheat straw	15-20	33-40	20-25
Switchgrass	5-20	30-50	10-40

2.2. Torrefaction

2.2.1. Introduction

Properties of raw biomass such as high oxygen and moisture content, hygroscopic nature, low bulk density and low calorific value, limit its use as a fuel [26]. Due to low energy density, high volume of biomass is needed in cogeneration plant, which can cause problems associated with storage, transportation, and feed handling. Furthermore, due to its tenacious and fibrous

structure, grinding biomass can be very costly, and in some cases impractical. All of these drawbacks have led to increased popularity of biomass torrefaction. Torrefaction is a thermal pre-treatment process in temperature that is carried out at temperature of 200 °C to 300 °C and for residence time of 15 min to 3 hr. It is carried out in a non-oxidizing environment at low heating rate (<50 ^{o}C/min) [27, 28]. During the process, the constitutive polymers of biomass partly decompose giving off various condensable and non-condensable gases. The final product is a carbon rich hydrophobic solid with high energy content, referred to as torrefied biomass. Energy efficiency of torrefaction process, defined as percent ratio between the energy yield in the product and the total energy (feedstock and process input) of up to 90% can be achieved in commercial process with most likely scenario being 80% or lower, depending on moisture content of biomass [26, 29]. Thermal efficiency can be increased by the use of gaseous and liquid products produced during torrefaction as an energy source for the process heat [29]. In addition, fibrous structure of biomass is broken down during torrefaction, which reduces the energy required to grind biomass significantly [29].

2.2.2. Characteristics of torrefied biomass

Most of previous studies on torrefaction have focused on physical characterization such as proximate and ultimate analyses, grindability, moisture adsorption, energy content of torrefied biomass. These properties are summarized below:

- Torrefaction is a drying process and thus, reduces the moisture content of biomass to less than 6% depending on the conditions of torrefaction [30].

- Torrefied biomass becomes hydrophobic and its moisture uptake is almost negligible even under severe storage conditions. This is due to destruction of the OH groups, causing the biomass to lose the capacity to form hydrogen bonds [31].
- Torrefaction causes biomass to become more porous resulting in significant reduction in its density [32].
- Biomass torrefied at optimum condition contains 70-80% of the original mass while retaining 80-90% of original energy, thus increasing the energy density by around 30% [29].
- Torrefaction reduces the O/C ratio through reduction in oxygen of biomass [33]. This makes a biomass better suited for gasification and pyrolysis and also increases its calorific value.
- Highly fibrous and tenacious nature of biomass is lost during torrefaction, increasing its grindability, flowability and handling characteristics [34]. The power consumption during grinding reduces dramatically (70-90%) when biomass is first torrefied [32].

2.2.3. Reactions and mechanisms

Differences in chemical structure of basic polymers of biomass (cellulose, hemicellulose and lignin) cause them to decompose at different temperature ranges and by different reaction mechanisms. Biomass torrefaction process can be divided into four different stages: moisture evaporation, hemicellulose decomposition, lignin decomposition and cellulose decomposition [27, 29]. The first stage, moisture removal or drying takes place at temperature less than 200 ^{o}C. Heating of biomass up to 100 ^{o}C removes the unbound water in biomass and further heating over 160 ^{o}C removes chemically bound water by thermo-condensation reaction which is accompanied

by release of CO_2 [29]. At temperature of 170 ^oC, devolatilization and carbonization of hemicellulose start. Extensive devolatilization of hemicellulose occurs at temperature 250 ^oC - 260 ^oC. The decomposition of the hemicellulose is accompanied by loss of large amount of water, CO_2, acetic acid, formaldehyde, furfural and formic acid [35, 36]. The energy values of these compounds are relatively low, which results in a significant increase in the energy content (MJ/kg) of the biomass [37]. Lignin decomposition has also been reported to start at 200 ^oC with relatively slower kinetics than hemicellulose and takes place at wide temperature range (up to 900 ^oC). Cellulose degradation is not very significant within the torrefaction temperature range (200 - 300 ^oC) and is reported to start at 270 ^oC and accelerates more noticeable at temperatures above 300 ^oC [29]. However, the decomposition characteristics of all biomass constituents also depend on biomass type and relative fraction of each component in biomass.

Most of the previous studies [26, 27, 30, 32, 33, 38] have focused on physical characterization of torrefied biomass such as density, energy value, moisture content and O/C ratio, and very little information is available on structural and chemical transformations of its major components during torrefaction. Few recent studies [23, 39, 40] have reported effect of torrefaction on structure of biomass components using ^{13}C NMR spectra. Advancement in ^{13}C NMR technique has enabled us to better understand the different linkages such as acetyl, aromatic, alkyl, glycosidic, methoxyl and ether in biomass components. A study carried out on torrefaction of bamboo reported that hemicellulose and cellulose degradation and structural changes in lignin macromolecule occur during torrefaction [40]. A number of studies [23, 39-41] have suggested the cleavage of β-O-4 linkages and increased aromaticity of lignin during thermal treatment. Increased aromaticity of torrefied biomass has been attributed to cleavage of lignin ether bonds [39, 42, 43] and decomposition of carbohydrates [39, 44] which could re-condense to form

aromatic C-C and C-H bonds. Melkior et al. [23] studied transformation of biomass constituents during torrefaction using ^{13}C NMR and identified the temperatures at which depolymerization of different components begin to occur. They reported that lignin is the first to be affected thermally when temperature rises above 200 ^{o}C, which causes demethoxylation of syringol components in lignin. β-O-4 linkage of lignin was reported to show significant cleavage above 245 ^{o}C. It is necessary to understand the structural changes in biomass polymers during torrefaction because it changes the reactions pathways of different polymers during fast pyrolysis process, hence affecting the composition of the final liquid product formed.

2.2.4. Factors affecting torrefaction

Torrefaction process parameters such as temperature, residence time and heating rate and biomass properties like particle size, initial moisture content and relative fraction of three major components affect properties of resulting torrefied biomass. Much research has been devoted for the study of torrefaction temperature and residence time on the energy and mass yield. Torrefaction temperature has shown to have more pronounced effect on mass and energy yield than residence time [45]. Heating rate in torrefaction is kept low and it is one of the aspects that make it different from fast pyrolysis process. Bergman et al. suggested limiting the heating rate of torrefaction at 50 ^{o}C/min [27]. However, no quantitative study on effects of heating rate is found till date. As torrefied wood can be ground using significantly less grinding energy, it is often desirable to torrefy the wood before grinding. However, very large particle size can cause problems associated with heat transfer and uniform heating. This limitation can be eliminated

using volumetric heating mechanism, such as microwave heating, where large biomass can be torrefied and then reduced in size as per the end use application requirement [32].

2.3. Fast pyrolysis

In fast pyrolysis process, biomass is heated rapidly (heating rate >500 ^{o}C/s) to moderate temperature (400-600 ^{o}C) to produce mostly vapors and aerosols and some charcoal and gas. After rapid cooling (vapor residence time = 1-2 sec), vapors and aerosols condense to form bio-oil. This gives high yields of liquid (up to 75 wt.%) which can be directly used in variety of applications [3]. A number of factors including process conditions such as reaction temperature and heat transfer rate, biomass properties and reactor configurations, play an important role in quality and yield of liquid formed from fast pyrolysis process.

The optimum temperature to maximize the liquid yield from lignocellulosic biomass has been reported to be 450-550 ^{o}C [46]. Exposure of biomass to lower temperature can favor the formation of undesirable charcoal. Liquid yields can be maximized with high heating rates and short vapor residence times to minimize secondary reactions [46]. To achieve very high heat and mass transfer rates, it is necessary to use finely ground biomass feed of particle size less than 3mm. Smaller particle size also assist in uniformly heating of biomass particles to bring it to optimum process temperature [47]. Liquid yield from fast pyrolysis also depends on char separation and biomass ash content, which have catalytic effect on vapor cracking. Moisture content in biomass is another important factor that affects the composition of liquid product from fast pyrolysis. Moisture in biomass is condensed in bio-oil as water and thereby negatively

affecting its fuel properties [22]. It is, therefore, necessary to dry the biomass to acceptable moisture content levels (~10 wt.%) [48].

Several types of reactors have been investigated in laboratory and commercial scale to produce bio-oil. Most common reactors used for fast pyrolysis process are: auger reactor, bubbling and circulation fluidized bed reactor, and ablative pyrolyser. Reactor configurations play an important role in heat and mass transfer rate and pyrolysis temperature, significantly affecting the distribution of compounds in bio-oil [48]. Several investigations have been carried out to determine the effect of temperature, vapor residence time, heating rate, particle size, moisture content and reactors configurations on the yield and quality of bio-oil produced [49-51]. Optimal operation parameters depend on biomass types and pyrolysis unit.

Py-GC/MS is a microscale analytical equipment, which has proven to be a powerful tool for separation and identification of compounds in pyrolytic vapor from lignocellulosic biomass. Azeez et al. [52] compared the composition of volatile pyrolysis products from Py-GC/MS and bio-oil formed from bench scale fluidized bed pyrolysis under similar conditions, and reported differences in the relative proportion of pyrolysis products. Smaller fraction of acids and non-aromatic aldehydes and ketones and larger fraction of lignin derivatives such as guaiacols and syringols were obtained from Py-GC/MS as compared to bio-oils from fluidized bed reactor [52]. From fast pyrolysis study of torrefied pine, Srinivasan et al. reported higher fraction of aromatic hydrocarbons and smaller fraction of furan compounds from Py-GC/MS as compared to bio-oils from fixed bed reactor [53]. Py-GC/MS has is typically employed to screen catalysts in regards to their ability to catalyze production of desirable hydrocarbons and other chemicals before larger-scale experimentation [54]. One of the drawbacks of the Py-GC/MS experiment is that it

does not allow product collection, and thus, the exact bio-oil yield could not be determined [55]. It also makes it difficult to detect heavier phenolic oligomers in bio-oil due to their limited volatility [56]. Py-GC/MS is used in this study because it provides convenient and quicker way to identify compounds in pyrolytic vapor.

2.4. Bio-oil characteristics

Characterization of bio-oils formed from variety of feedstock and process conditions have been performed to determine it physical properties such as density, pH, water content, heating value and elemental analysis. The important characteristics of bio-oil based on a review article are summarized below [57]:

- Bio-oil has high oxygen content usually in the range of 35-40 wt.%.
- Water content of bio-oil usually ranges from 15-30 wt. %. Water ends up in the bio-oil either from original moisture in biomass feed or as by-product of dehydration reactions taking place during pyrolysis.
- Bio-oil is acidic in nature (pH = 2-3).
- The viscosity of bio-oil varies over a wide range (35-1000 cP at 40 ^{o}C) and decreases at higher temperature. It also depends on feedstock and process conditions.
- Bio-oil is unstable and when they are stored for long time, its viscosity increases possibly due to reactions among various compounds in bio-oil.

These properties of bio-oil have significant impact on its combustion behaviors for energy applications and limit its use. The major drawback is the high oxygen content, which is the cause

of major differences between bio-oil and hydrocarbon fuels. This high fraction of oxygen is responsible for the low heating value (16-19 MJ/kg) of bio-oil, which is half of the heating value of conventional fuel oils. Presence of highly reactive oxygenated compounds such as aldehydes, ketones and phenols makes the bio-oil unstable and causes aging. Due to its complex composition, the boiling point of bio-oil varies over a wide range. In addition, slow heating of bio-oil during distillation causes polymerization of reactive components, leaving 35-50% of reactive material as residue. Presence of water lowers the viscosity of bio-oil thus, improving its flow characteristics. On the other hand, it also causes low heating value and flame temperature, greater ignition delay and lower combustion rate of bio-oil. High acidity of bio-oil is due to presence of organic acids, mainly, carboxylic acid and formic acid that make it corrosive to common construction materials such as carbon steel and aluminum. The oxygen in bio-oil must be removed via various upgrading techniques before they can be used as replacement for gasoline and diesel.

2.5. Fast pyrolysis chemistry and product distribution

Pyrolysis of cellulose, hemicellulose and lignin has been carried out separately to study the chemistry and reaction mechanisms involved with depolymerization and decomposition of the individual components. Much focus has been given to thermogravimetric and differential scanning calorimetry techniques to study the mass loss kinetics and to quantify products yields as char, tar, and gases. These three components of biomass are reported to decompose independently of each other and the volatiles are evolved from cellulose and hemicellulose while char is mainly produced from lignin [58, 59]

Decomposition of cellulose during fast pyrolysis (at temperature >270 ^{o}C) first involves its transformation to liquid. Then, it either directly decomposes to form certain smaller sized molecular products such as furan, levoglucosan, glycolaldehyde and hydroxyl acetone, or forms two-degree oligomers. The oligomers can further breakdown to form furan, light oxygenates, char, permanent gases and levoglucosan [24, 60, 61]. Levoglucosan is the major product from the pyrolysis of cellulose [15] and altogether 27 different compounds have been identified [62]. The char yield from cellulose is found to increase due to secondary reactions among the primary degradation products. Re-polymerization and secondary pyrolysis of levoglucosan was also found to be an important pathway for char formation [63].

Hemicellulose decomposes between 220 ^{o}C and 315 ^{o}C and the main products identified are water, methanol, formic, acetic, propionic acids, hydroxyl-1-propanon, hydroxyl-1-butanon, 2-methylfuran, 2-furfuraldehyde, dianhydroxylo-pyranose, and anhydroxylopyranose [24, 64]. Pure hemicellulose is also reported to produce more char yield (10.7 wt. %) than cellulose (5%) [64]. However, in pyrolysis of biomass, char yield greatly depend on ash content as it can catalyze the formation of char.

The first step in pyrolysis of lignin is dehydration which starts at about 200 ^{o}C, followed by cleavage of β-O-4 linkage at 250-350 ^{o}C forming forms guaiacol, dimethoxyphenol, dimethoxyacetophenone, and trimethoxyacetophenone [24, 65]. Breakdown of α-, and β-aryl-alkyl-ether linkages take place between 150 ^{o}C and 300 ^{o}C and aliphatic side chains split up from aromatic ring at 300 ^{o}C. Higher temperature (370-400 ^{o}C) is required to break the C-C bond between lignin structural units [24, 66]. The bond cleavage of lignin during pyrolysis has been categorized three types: Firstly, cleavage of methyl C-O bond to form products with two oxygen

atoms; Secondly, cleavage of C-O bond to form one-oxygen atom product and lastly, cleavage of C-C side bond cleavage which forms guaiacol and pyrogallol, the relative abundance of which depends on the type of biomass [24]. Phenolic compounds are the main product from lignin pyrolysis.

The chemical composition of bio-oil has been widely studied by using GC/MS and about 300 different types of compounds have been identified which include aldehydes, ketones, carboxylic acids, furan/pyran, esters, phenolic compounds, anhydrosugars, and other oxygenated compounds [24, 62, 67, 68]. The chemical composition of bio-oil grouped according to their functional group and their relative abundance is shown in Figure 2.3 [69].

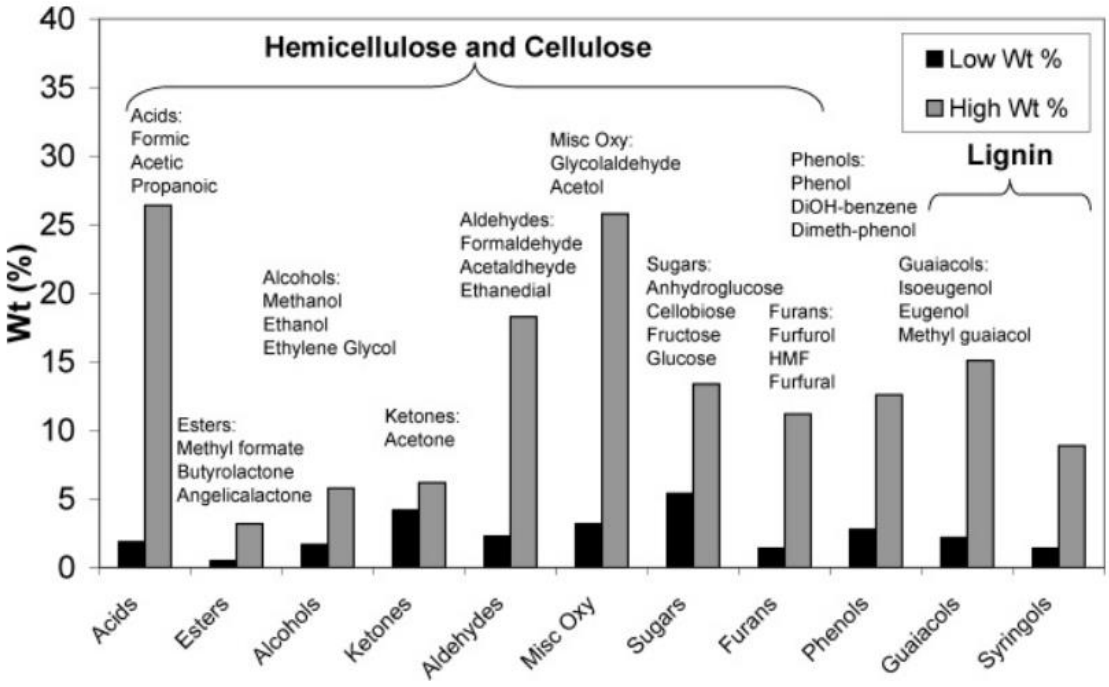

Figure 2.3 Bio-oil compounds and their relative abundance [69]

2.6. Catalytic fast pyrolysis

A number of techniques have been explored to upgrade bio-oil so that it can be blended with transportation fuel. Upgrading of bio-oil involves its deoxygenation to remove oxygenated compounds and cracking to break the high-molecular weight compounds into smaller compounds. Hydrodeoxygenation process has been explored in great detail to upgrade bio-oil. It is carried out at temperature 230-500 ^{o}C and pressure 50-200 psi in the presence of heterogeneous catalysts to remove oxygen from bio-oil as water [70]. However, high oxygen content in bio-oil leads to extremely high hydrogen consumption (~6 kg of H_2/100 kg of bio-oil) which impairs process economics [71]. An alternative to hydrodeoxygenation is catalytic fast pyrolysis (CFP) process.

In CFP, bio-oil compounds are deoxygenated in the presence of some shape-selective catalysts such as zeolites. It involves the rupture of C-C bonds associated with dehydration, decarboxylation, and decarbonylation, and produces aromatic compounds. CFP can either be *in-situ*, in which biomass and catalyst are mixed together and pyroyzed or *ex-situ* upgrading where only the pyrolysis vapors comes in contact with the catalyst. The *in-situ* catalytic pyrolysis of biomass feedstock allows the conversion of biomass into highly de-oxygenated bio-oil in a single step. Microporous catalyst, particularly H^{+}ZSM-5 has been extensively studied to upgrade pyrolytic vapor due to its strong acidity and shape selectivity. It has good thermal and hydrothermal stability and is most effective catalyst for aromatic hydrocarbon production from the pyrolytic vapor [72-74].

The reaction mechanism for catalytic fast pyrolysis of cellulose, hemicellulose and lignin using H^{+}ZSM-5 has been proposed by previous studies [75-78]. During pyrolysis of cellulose, it first

decomposes to form anhydrosugar (primarily levoglucosan). Dehydration of levoglucosan takes place to form furans, which undergo series of dehydration, oligomerization, decarbonylation and decarboxylation reactions inside the pores of zeolites to form aromatics and olefins. At the same time, recondensation and polymerization reactions among cellulose degradation products can also occur which forms char and low molecular oxygenates [75, 78, 79]. Decomposition of hemicellulose produces pyrans and furans [64], which can also diffuse into the pores of zeolite to form aromatic and olefins. During CFP of lignin, it either decomposes to form phenolic compounds or undergo polycondensation to form char. Phenols can also be converted into aromatics in the pores of zeolite catalyst [75, 78, 79]. The major problem with zeolites is low liquid yield as much of the bio-oil will convert into coke [77, 80, 81]. The catalyst can be regenerated and reused after the upgrading process. However, continuous regeneration of catalyst resulted in its poor efficiency in producing aromatics; furthermore, after few runs the regenerated catalyst becomes totally deactivated with loss of acidic sites [82].

2.7. Fast pyrolysis of biomass pretreated by torrefaction

Recent studies [53, 83-91] have investigated torrefied biomass for production of bio-oil from fast pyrolysis process. These studies have mainly focused on bio-oil characterization such as O/C ratios, acid and water content, heating values, liquid yield and chemical composition. Meng et al. carried out fast pyrolysis study on torrefied loblolly pine and reported improved oxygen to carbon ratio in bio-oil [86]. Zheng et al. also investigated the quality of bio-oil produce from torrefied pine and reported improvement in its quality by reduction of water and acetic acid content and increase in aromaticity and higher heating value of bio-oil [89]. In both cases, the

improvement in quality of bio-oil was achieved with the penalty of decrease in yield of bio-oil. Decrease in bio-oil yield when torrefied biomass was used instead of raw biomass was attributed to cross linking and charring during torrefaction as revealed by ^{13}C NMR and FTIR analysis of torrefied corncobs [90]. Several studies [83, 88-90] reported increase in yield of phenolic compounds when torrefied biomass was used instead of raw, while Srinivasan et al. [53] reported no significant change in phenolic yield due to torrefaction pretreatment. Increase in anhydrous sugar has also been reported which due to increase fraction of cellulose in biomass [88, 91]. Guaiacol compounds have been reported to increase [53, 91] or decrease [87] with torrefaction. Torrefied biomass has lower oxygen to carbon ratio, which can result in bio-oil with lower oxygenated compounds. Also, at mild torrefaction condition, hemicellulose component of biomass evolves as volatile; as a result yield of hemicellulose derivatives like organic acids and furan compounds in bio-oil decrease.

Very few recent articles [53, 84, 85, 92-94] have investigated the effect of torrefaction pretreatment on catalytic pyrolysis using H^+ZSM-5. Srinivasan et al. studied the catalytic pyrolysis of pine wood torrefied at 225 ^oC and 30 min and found significant increase in yield of aromatic hydrocarbons and total carbon yield [53]. Another study from the same group has also shown in increased aromatic HC when torrefied lignin was used instead of raw lignin [92]. Recent study carried out on catalytic pyrolysis of torrefied corncobs at different severity has also reported that torrefaction can serve as an effective method to improve BTX selectivity [94]. Due to differences in experimental conditions of torrefaction and pyrolysis in different studies, no clear conclusion can be drawn in predicting the biomass characteristics that are important in hydrocarbon production. Clear understanding on how torrefaction causes changes in biomass constitutive polymers: cellulose, hemicellulose and lignin and how that subsequently affects the

product yield from fast pyrolysis are not yet understood. Therefore, this study aims to bridge the gap in the existing literature that fails to acknowledge the effect of changes in biomass structure during torrefaction in product distribution from non-catalytic and catalytic pyrolysis. The findings from this study can also be applied to other biomass feedstock to determine the optimum torrefaction condition that can maximize hydrocarbon yield from H^+ZSM-5 catalyzed fast pyrolysis.

2.8. References

1. Stevens, C. and R.C. Brown, *Thermochemical processing of biomass: conversion into fuels, chemicals and power*. Vol. 12. 2011: John Wiley & Sons.

2. Bridgwater, A., D. Meier, and D. Radlein, *An overview of fast pyrolysis of biomass.* Organic Geochemistry, 1999. **30**(12): p. 1479-1493.

3. Bridgwater, A., *Renewable fuels and chemicals by thermal processing of biomass.* Chemical Engineering Journal, 2003. **91**(2): p. 87-102.

4. Wyman, C.E., *Alternative fuels from biomass and their impact on carbon dioxide accumulation.* Applied Biochemistry and Biotechnology, 1994. **45**(1): p. 897-915.

5. Ramos, L.P., *The chemistry involved in the steam treatment of lignocellulosic materials.* Química Nova, 2003. **26**(6): p. 863-871.

6. Sluiter, A., et al., *Determination of extractives in biomass.* Laboratory Analytical Procedure (LAP), 2005. **1617**.

7. Lynd, L.R., et al., *Fuel ethanol from cellulosic biomass.* Science(Washington), 1991. **251**(4999): p. 1318-1323.

8. Ghosh, P. and A. Singh, *Physiochemical and biological treatments for enzymatic/microbial conversion of lignocellulosic biomass.* Advances in Applied Microbiology, 1993. **39**: p. 295-333.

9. Gardner, K. and J. Blackwell, *The hydrogen bonding in native cellulose.* Biochimica et Biophysica Acta (BBA)-General Subjects, 1974. **343**(1): p. 232-237.

10. Knauf, M. and M. Moniruzzaman, *Lignocellulosic biomass processing: a perspective.* International Sugar Journal, 2004. **106**(1263): p. 147-150.

11. Cabiac, A., et al., *Cellulose reactivity and glycosidic bond cleavage in aqueous phase by catalytic and non catalytic transformations.* Applied Catalysis A: General, 2011. **402**(1–2): p. 1-10.

12. Fan, L., Y.H. Lee, and D. Beardmore, *The influence of major structural features of cellulose on rate of enzymatic hydrolysis.* Biotechnology and Bioengineering, 1981. **23**(2): p. 419-424.

13. Lynd, L.R., et al., *Microbial cellulose utilization: fundamentals and biotechnology.* Microbiology and Molecular Biology Reviews, 2002. **66**(3): p. 506-577.

14. Lee, S.B., et al., *Structural properties of cellulose and cellulase reaction mechanism.* Biotechnology and Bioengineering, 1983. **25**(1): p. 33-51.

15. Patwardhan, P.R., et al., *Product distribution from fast pyrolysis of glucose-based carbohydrates.* Journal of Analytical and Applied Pyrolysis, 2009. **86**(2): p. 323-330.

16. Poutanen, K., J. Puls, and M. Linko, *The hydrolysis of steamed birchwood hemicellulose by enzymes produced byTrichoderma reesei andAspergillus awamori.* Applied Microbiology and Biotechnology, 1986. **23**(6): p. 487-490.

17. Boerjan, W., J. Ralph, and M. Baucher, *Lignin biosynthesis.* Annual Review of Plant Biology, 2003. **54**(1): p. 519-546.

18. Kubicek, C.P., *Fungi and lignocellulosic biomass*. 2012: John Wiley & Sons.

19. Adler, E., *Lignin chemistry—past, present and future.* Wood Science and Technology, 1977. **11**(3): p. 169-218.

20. Sjöström, E., *Wood chemistry: fundamentals and applications*. 1993: Gulf Professional Publishing.

21. Patwardhan, P.R., R.C. Brown, and B.H. Shanks, *Understanding the fast pyrolysis of lignin.* ChemSusChem, 2011. **4**(11): p. 1629-1636.

22. Mohan, D., C.U. Pittman, and P.H. Steele, *Pyrolysis of Wood/Biomass for Bio-oil: A Critical Review*. Energy & Fuels, 2006. **20**(3): p. 848-889.

23. Melkior, T., et al., *NMR analysis of the transformation of wood constituents by torrefaction.* Fuel, 2012. **92**(1): p. 271-280.

24. Liu, C., et al., *Catalytic fast pyrolysis of lignocellulosic biomass.* Chemical Society Reviews, 2014. **43**(22): p. 7594-7623.

25. McKendry, P., *Energy production from biomass (part 1): overview of biomass.* Bioresource Technology, 2002. **83**(1): p. 37-46.

26. Arias, B., et al., *Influence of torrefaction on the grindability and reactivity of woody biomass.* Fuel Processing Technology, 2008. **89**(2): p. 169-175.

27. Bergman, P., et al., *Torrefaction for biomass co-firing in existing coal-fired power stations.* Energy Centre of Netherlands, Report No. ECN-C-05-013, 2005.

28. Pentananunt, R., A. Rahman, and S. Bhattacharya, *Upgrading of biomass by means of torrefaction.* Energy, 1990. **15**(12): p. 1175-1179.

29. Van der Stelt, M., et al., *Biomass upgrading by torrefaction for the production of biofuels: a review.* Biomass and Bioenergy, 2011. **35**(9): p. 3748-3762.

30. Lipinsky, E.S., J.R. Arcate, and T.B. Reed, *Enhanced wood fuels via torrefaction.* Fuel Chemistry division preprints, 2002. **47**(1): p. 408-410.

31. Pastorova, I., P.W. Arisz, and J.J. Boon, *Preservation of D-glucose-oligosaccharides in cellulose chars.* Carbohydrate Research, 1993. **248**: p. 151-165.

32. Bergman, P.C. and J.H. Kiel. *Torrefaction for biomass upgrading*. in *Proc. 14th European Biomass Conference, Paris, France*. 2005.

33. Chad, L.C., et al., *Physicochemical Properties of Thermally Treated Biomass and Energy Requirement for Torrefaction.* Transactions of the ASABE, 2013. **56**(3).

34. Tumuluru, J.S., et al., *Biomass torrefaction process review and moving bed torrefaction system model development*. 2010, Idaho National Laboratory (INL).

35. Weiland, J., R. Guyonnet, and R. Gibert, *Analysis of controlled wood burning by combination of thermogravimetric analysis, differential scanning calorimetry and Fourier transform infrared spectroscopy.* Journal of Thermal Analysis and Calorimetry, 1998. **51**(1): p. 265-274.

36. Weiland, J.-J. and R. Guyonnet, *Study of chemical modifications and fungi degradation of thermally modified wood using DRIFT spectroscopy.* Holz als Roh-und Werkstoff, 2003. **61**(3): p. 216-220.

37. Zanzi Vigouroux, R., et al. *Biomass torrefaction*. in *2nd World Conf. on Biomass for Energy, Industry and Climate Protection*. 2004.

38. Bergman, P., *Combined torrefaction and pelletisation.* The TOP process, 2005.

39. Ben, H. and A.J. Ragauskas, *Torrefaction of Loblolly pine.* Green Chemistry, 2012. **14**(1): p. 72-76.

40. Wen, J.-L., et al., *Understanding the chemical and structural transformations of lignin macromolecule during torrefaction.* Applied Energy, 2014. **121**: p. 1-9.

41. Sharma, R.K., et al., *Characterization of chars from pyrolysis of lignin.* Fuel, 2004. **83**(11): p. 1469-1482.

42. Ben, H. and A.J. Ragauskas, *NMR characterization of pyrolysis oils from Kraft lignin.* Energy & Fuels, 2011. **25**(5): p. 2322-2332.

43. Britt, P.F., et al., *Flash vacuum pyrolysis of methoxy-substituted lignin model compounds.* The Journal of Organic Chemistry, 2000. **65**(5): p. 1376-1389.

44. Zawadzki, J. and M. Wisniewski, *^{13}C NMR study of cellulose thermal treatment.* Journal of Analytical and Applied Pyrolysis, 2002. **62**(1): p. 111-121.

45. Repellin, V., et al., *Modelling anhydrous weight loss of wood chips during torrefaction in a pilot kiln.* Biomass and Bioenergy, 2010. **34**(5): p. 602-609.

46. Bridgwater, A., *Principles and practice of biomass fast pyrolysis processes for liquids.* Journal of Analytical and Applied Pyrolysis, 1999. **51**(1): p. 3-22.

47. Bridgwater, A. and G. Peacocke, *Fast pyrolysis processes for biomass.* Renewable and Sustainable Energy Reviews, 2000. **4**(1): p. 1-73.

48. Bridgwater, A.V., S. Czernik, and J. Diebold, *Fast pyrolysis of biomass: a handbook*. Vol. 1. 1999: Cpl Pr.

49. Fahmi, R., et al., *The effect of lignin and inorganic species in biomass on pyrolysis oil yields, quality and stability.* Fuel, 2008. **87**(7): p. 1230-1240.

50. DEMİRBAŞ, A., *Bioethanol from cellulosic materials: a renewable motor fuel from biomass.* Energy Sources, 2005. **27**(4): p. 327-337.

51. Garcia-Perez, M., et al., *Effects of temperature on the formation of lignin-derived oligomers during the fast pyrolysis of mallee woody biomass.* Energy & fuels, 2008. **22**(3): p. 2022-2032.

52. Azeez, A.M., et al., *Fast pyrolysis of African and European lignocellulosic biomasses using Py-GC/MS and fluidized bed reactor.* Energy & Fuels, 2010. **24**(3): p. 2078-2085.

53. Srinivasan, V., et al., *Catalytic pyrolysis of torrefied biomass for hydrocarbons production.* Energy & Fuels, 2012. **26**(12): p. 7347-7353.

54. Mullen, C.A. and A.A. Boateng, *Catalytic pyrolysis-GC/MS of lignin from several sources.* Fuel Processing Technology, 2010. **91**(11): p. 1446-1458.

55. Lu, Q., et al., *Selective fast pyrolysis of biomass impregnated with ZnCl2 to produce furfural: Analytical Py-GC/MS study.* Journal of Analytical and Applied Pyrolysis, 2011. **90**(2): p. 204-212.

56. Bai, X., et al., *Formation of phenolic oligomers during fast pyrolysis of lignin.* Fuel, 2014. **128**: p. 170-179.

57. Czernik, S. and A. Bridgwater, *Overview of applications of biomass fast pyrolysis oil.* Energy & Fuels, 2004. **18**(2): p. 590-598.

58. Williams, P.T. and S. Besler, *The pyrolysis of rice husks in a thermogravimetric analyser and static batch reactor.* Fuel, 1993. **72**(2): p. 151-159.

59. Nunn, T.R., et al., *Product compositions and kinetics in the rapid pyrolysis of milled wood lignin.* Industrial & Engineering Chemistry Process Design and Development, 1985. **24**(3): p. 844-852.

60. Mettler, M.S., et al., *Revealing pyrolysis chemistry for biofuels production: Conversion of cellulose to furans and small oxygenates.* Energy & Environmental Science, 2012. **5**(1): p. 5414-5424.

61. Luo, Z., et al., *Mechanism study of cellulose rapid pyrolysis.* Industrial & Engineering Chemistry Research, 2004. **43**(18): p. 5605-5610.

62. Zhang, J., et al., *Product analysis and thermodynamic simulations from the pyrolysis of several biomass feedstocks.* Energy & Fuels, 2007. **21**(4): p. 2373-2385.

63. Kawamoto, H., M. Murayama, and S. Saka, *Pyrolysis behavior of levoglucosan as an intermediate in cellulose pyrolysis: polymerization into polysaccharide as a key reaction to carbonized product formation.* Journal of Wood Science, 2003. **49**(5): p. 469-473.

64. Patwardhan, P.R., R.C. Brown, and B.H. Shanks, *Product distribution from the fast pyrolysis of hemicellulose.* ChemSusChem, 2011. **4**(5): p. 636-643.

65. Hwang, B.-h. and J.R. Obst. *Basic studies on the pyrolysis of lignin compounds*. in *Proceedings of the IAWPS International Conference on Forest Products: Better Utilization of Wood for Human, Earth and Future. The Korean Society of Wood Science and Technology International Association of Wood Products Societies, Daejeon, Korea*. 2003.

66. Balat, M., *Mechanisms of thermochemical biomass conversion processes. Part 1: reactions of pyrolysis.* Energy Sources, Part A, 2008. **30**(7): p. 620-635.

67. Venderbosch, R. and W. Prins, *Fast pyrolysis technology development.* Biofuels, bioproducts and biorefining, 2010. **4**(2): p. 178-208.

68. Mortensen, P.M., et al., *A review of catalytic upgrading of bio-oil to engine fuels.* Applied Catalysis A: General, 2011. **407**(1): p. 1-19.

69. Huber, G.W., S. Iborra, and A. Corma, *Synthesis of transportation fuels from biomass: chemistry, catalysts, and engineering.* Chemical reviews, 2006. **106**(9): p. 4044-4098.

70. Xiu, S. and A. Shahbazi, *Bio-oil production and upgrading research: A review.* Renewable and Sustainable Energy Reviews, 2012. **16**(7): p. 4406-4414.

71. Marinangeli, R., et al., *Opportunities for biorenewables in oil refineries.* Department of Energy Final Technical Report, US Department of Energy: Des Plaines, 2005.

72. Adjaye, J. and N. Bakhshi, *Production of hydrocarbons by catalytic upgrading of a fast pyrolysis bio-oil. Part I: Conversion over various catalysts.* Fuel Processing Technology, 1995. **45**(3): p. 161-183.

73. Jae, J., et al., *Investigation into the shape selectivity of zeolite catalysts for biomass conversion.* Journal of Catalysis, 2011. **279**(2): p. 257-268.

74. Mihalcik, D.J., C.A. Mullen, and A.A. Boateng, *Screening acidic zeolites for catalytic fast pyrolysis of biomass and its components.* Journal of Analytical and Applied Pyrolysis, 2011. **92**(1): p. 224-232.

75. Carlson, T.R., et al., *Production of green aromatics and olefins by catalytic fast pyrolysis of wood sawdust.* Energy & Environmental Science, 2011. **4**(1): p. 145-161.

76. Carlson, T.R., et al., *Catalytic fast pyrolysis of glucose with HZSM-5: the combined homogeneous and heterogeneous reactions.* Journal of Catalysis, 2010. **270**(1): p. 110-124.

77. Carlson, T.R., T.P. Vispute, and G.W. Huber, *Green gasoline by catalytic fast pyrolysis of solid biomass derived compounds.* ChemSusChem, 2008. **1**(5): p. 397-400.

78. Zheng, A., et al., *Effect of crystal size of ZSM-5 on the aromatic yield and selectivity from catalytic fast pyrolysis of biomass.* Journal of Molecular Catalysis A: Chemical, 2014. **383–384**(0): p. 23-30.

79. Carlson, T.R., et al., *Aromatic production from catalytic fast pyrolysis of biomass-derived feedstocks.* Topics in Catalysis, 2009. **52**(3): p. 241-252.

80. Gayubo, A.G., et al., *Transformation of oxygenate components of biomass pyrolysis oil on a HZSM-5 zeolite. I. Alcohols and phenols.* Industrial & Engineering Chemistry Research, 2004. **43**(11): p. 2610-2618.

81. Gayubo, A.G., et al., *Transformation of oxygenate components of biomass pyrolysis oil on a HZSM-5 zeolite. II. Aldehydes, ketones, and acids.* Industrial & Engineering Chemistry Research, 2004. **43**(11): p. 2619-2626.

82. Vitolo, S., et al., *Catalytic upgrading of pyrolytic oils over HZSM-5 zeolite: behaviour of the catalyst when used in repeated upgrading–regenerating cycles.* Fuel, 2001. **80**(1): p. 17-26.

83. Boateng, A.A. and C.A. Mullen, *Fast pyrolysis of biomass thermally pretreated by torrefaction.* Journal of Analytical and Applied Pyrolysis, 2013. **100**(0): p. 95-102.

84. Hilten, R.N., et al., *Effect of torrefaction on bio-oil upgrading over HZSM-5. Part 1: Product yield, product quality, and catalyst effectiveness for benzene, toluene, ethylbenzene, and xylene production.* Energy & Fuels, 2013. **27**(2): p. 830-843.

85. Hilten, R.N., et al., *Effect of torrefaction on bio-oil upgrading over HZSM-5. Part 2: Byproduct formation and catalyst properties and function.* Energy & Fuels, 2012. **27**(2): p. 844-856.

86. Meng, J., et al., *The effect of torrefaction on the chemistry of fast-pyrolysis bio-oil.* Bioresource Technology, 2012. **111**(0): p. 439-446.

87. Ren, S., et al., *The effects of torrefaction on compositions of bio-oil and syngas from biomass pyrolysis by microwave heating.* Bioresource Technology, 2013. **135**: p. 659-664.

88. Yang, Z., et al., *Effects of torrefaction and densification on switchgrass pyrolysis products.* Bioresource Technology, 2014.

89. Zheng, A., et al., *Effect of torrefaction temperature on product distribution from two-staged pyrolysis of biomass.* Energy & Fuels, 2012. **26**(5): p. 2968-2974.

90. Zheng, A., et al., *Effect of torrefaction on structure and fast pyrolysis behavior of corncobs.* Bioresource Technology, 2013. **128**(0): p. 370-377.

91. Branca, C., et al., *Effects of the torrefaction conditions on the fixed-bed pyrolysis of Norway spruce.* Energy & Fuels, 2014. **28**(9): p. 5882-5891.

92. Adhikari, S., V. Srinivasan, and O. Fasina, *Catalytic pyrolysis of raw and thermally treated lignin using different acidic zeolites.* Energy & Fuels, 2014. **28**(7): p. 4532–4538.

93. Srinivasan, V., et al., *Catalytic pyrolysis of raw and thermally treated cellulose using different acidic zeolites.* BioEnergy Research, 2014. **7**(3): p. 867-875.

94. Zheng, A., et al., *Catalytic fast pyrolysis of biomass pretreated by torrefaction with varying severity.* Energy & Fuels, 2014. **28**(9): p. 5804-5811.

3. Effect of Torrefaction on Biomass Structure and Hydrocarbons Production from Fast Pyrolysis

3.1. Abstract

Torrefaction has been shown to improve the chemical composition of bio-oil produced from fast pyrolysis by lowering its oxygen content and enhancing aromatic yield. Py-GC/MS study was employed to investigate the effect of torrefaction temperatures (225, 250 and 275 ^{o}C) and residence times (15, 30 and 45 min) on product distribution from non-catalytic and H^{+}ZSM-5 catalyzed pyrolysis of pinewood. During torrefaction, structural transformations in biomass constitutive polymers: hemicellulose, cellulose and lignin took place, which were evaluated using component analysis, solid state CP/MAS ^{13}C NMR and XRD techniques. Torrefaction caused deacetylation and decomposition of hemicellulose, cleavage of aryl ether linkages and demethoxylation of lignin, degradation of cellulose and overall increase in aromaticity of biomass, all of which affected the product yield from pyrolysis of torrefied biomass. For non-catalytic pyrolysis, selectivity of phenolic compounds increased with increase in torrefaction severity while that of furan compounds decreased. In the case of catalytic pyrolysis, sample torrefied at 225^{o}C-30min and 250^{o}C-15min resulted in significant increase in aromatic HC and also total carbon yield (approx. 1.6 times higher) as compared to catalytic pyrolysis of non-torrefied pine. Cleavage of aryl ether linkages and demethoxylation in lignin due to torrefaction caused increased yield of phenolic compounds, which in presence of catalyst were dehydrated to from aromatic HC.

Keywords: *Torrefaction, Fast pyrolysis, Catalytic pyrolysis, ZSM-5, CP MAS* ^{13}C *NMR, Pinewood*

3.2. Introduction

Dwindling fossil fuel sources and dependence of the United States on foreign oil have led to calls for an increased use of locally available energy sources such as biomass in lieu of fossil fuels. Biomass can be converted into bio-oil by fast pyrolysis process, during which organic compounds in biomass encounter rapid thermal decomposition in the absence of oxygen [1]. Bio-oils produced from fast pyrolysis have negligible content of sulfur, nitrogen and ash, and thus, allow relatively cleaner combustion than conventional petroleum oil. Bio-oils have been successfully used as boiler fuel, serve as a major source of chemicals such as methanol, turpentine and acetic acid, and have shown promise in diesel engine and gas turbine applications[2]. However, high acidity, low heating values and high oxygen and water contents in bio-oils render them unsuitable as a transport fuel. The primary issue is the high oxygen content (usually 35–40%) [2, 3], which leads to lower energy content and immiscibility with hydrocarbon fuels. In addition, the strong acidity of bio-oils makes them extremely unstable. A number of approaches such as fast pyrolysis process optimization, catalytic pyrolysis and catalytic upgrading of pyrolysis vapors have been used to improve the quality of bio-oil in terms of chemical composition. In addition, thermal pretreatment of biomass, i.e., torrefaction, has also shown to improve the quality of bio-oil by lowering its acidity and increasing energy content[4]. Recent studies have shown that torrefaction also improves the chemical composition of bio-oil by lowering oxygen content and enhancing aromatic yield [5-12].

Torrefaction is a mild pyrolysis in which biomass is heated to 200-300 °C in an inert environment. As a result, hemicellulose is decomposed and volatile gases and moisture are driven off. The resulting solid has better fuel properties due to increase in energy content (MJ/kg) and grindability and decrease in moisture and O/C ratio [13, 14]. Few recent studies have reported that torrefaction not only causes physical changes in biomass but also structural transformations in its major components: cellulose, hemicellulose and lignin [8, 15-18]. Cellulose is a linear polymer composed of D-glucose subunits arranged in crystalline structure of microfibrils [19] and is resistant to thermal decomposition. Hemicellulose is the least thermally stable composition [20] among biomass components, which is composed primarily of xylans and mannans [21]. Lignin is a three-dimensional, highly branched, polyphenolic substance that is generally composed of p-hydroxyphenyl, syringyl and guaiacyl units [22, 23], with their composition depending on the plant species, and has very high thermal stability [20]. The three lignin monomers are interconnected with different type of linkages: β-O-4, β-β, 5-5, β-5 and 4-O-5 of which, the β-O-4 (aryl glycerol-β-aryl ether) creates the most abundant structure, generally involving 50% and 60% of phenylpropanoid units in softwood and hardwood lignin, respectively [24]. A study carried out on torrefaction of bamboo reported that hemicellulose and cellulose degradation and structural changes in lignin macromolecule occur during torrefaction [15]. A number of studies have suggested the cleavage of β-O-4 linkages and increase in aromaticity of lignin during torrefaction [15-17, 25]. However, the effect of this chemical transformation on product distribution from non-catalytic and catalytic pyrolysis of torrefied biomass has not been understood so far. Srinivasan et al. studied catalytic pyrolysis of torrefied biomass using H^{+}ZSM-5 catalyst, and has demonstrated that aromatic hydrocarbons such as benzene, toluene and xylene (BTX compounds) in bio-oil can be doubled when torrefied biomass

is used instead of raw biomass [5]. In the presence of acidic zeolites catalyst like H^+ZSM-5, oxygenated bio-oil compounds undergo a series of decarbonylation, decarboxylation, dehydration and oligomerization reactions to form aromatic compound [26]. However, the role of zeolite catalyst in pyrolysis of torrefied biomass has not been understood. Therefore, the objective of the present study was to develop fundamental understanding on chemical and structural transformations of biomass components during torrefaction and quantify the impacts of these transformations on hydrocarbons production from non-catalytic and catalytic fast pyrolysis.

Thus, in this study, loblolly pine samples torrefied under different conditions were characterized (using component analysis, CP-MAS ^{13}C NMR spectra and XRD techniques) and pyrolyzed (without and with catalyst) using Py-GC/MS. It is believed that variations in product distribution and yield from fast pyrolysis of the samples could be better explained in terms of biomass characteristics. The governing hypothesis of this study is that structural changes in biomass components as a result of torrefaction can increase aromatic yield during biomass pyrolysis.

3.3. Material and Methods

3.3.1. Material and sample preparation

Loblolly pine used for this study was obtained from the Mary Olive Thomas Research Forest of Auburn University (Auburn, Alabama). Pinewood was torrefied at three temperatures (225, 250 and 275 ^oC) and for three residence times (15, 30 and 45 min) for a total of 9 treatments. The nomenclature used in the present study for samples torrefied at different conditions is given in Table 3.1.

Table 3.1 Nomenclature used for samples torrefied at different conditions

Nomenclature	Torrefaction Temperature (^{o}C)	Torrefaction Residence Time (min)
Control	Non-torrefied (raw) pine	
225^{o}C-15min	225	15
225^{o}C-30min	225	30
225^{o}C-45min	225	45
250^{o}C-15min	250	15
250^{o}C-30min	250	30
250^{o}C-45min	250	45
275^{o}C-15min	275	15
275^{o}C-30min	275	30
275^{o}C-45min	275	45

Treatments were conducted in a Thermo Scientific furnace purged with nitrogen gas, using open top aluminum pans. Detailed procedure used for torrefaction and sample preparation can be found elsewhere [13]. Results of physical and chemical characterization that include proximate and ultimate analyses, mass loss during torrefaction and energy content of torrefied biomass are also given in the same study [13]. Briefly, they are summarized in Table 3.2. For the given torrefaction range, the total percent solids retained decreased (97.96% to 46.67%) with increase in torrefaction temperature and time. It was reported in the study that effect of residence time on solid yield was more significant (accounting 42% of variation) than temperature. The bulk density of torrefied biomass also decreased as the biomass became more porous due to torrefaction. It is also observed that ash contents of the treated samples increased while volatiles decreased as the temperature and residence time of torrefaction was increased. Energy content for the biomass also increased with torrefaction parameters. The initial energy content was 20.18 MJ/kg and it increased to 26.68 MJ/kg at the most intense torrefaction condition. The higher

carbon percentage and lower oxygen percentage of torrefied sample can cause increase in heating value of the samples.

Table 3.2 Physical and chemical properties of torrefied loblolly pine (dry basis) [13]

Sample	Solid retained (wt. %)	Bulk density (kg/m^3)	Moisture %	Ash %	Volatile %	C %	O %	HHV (MJ/kg)
Control	-	159.2	6.22	0.72	80.79	50.9	41.84	20.18
225°C-15min	97.96	146.4	6.07	0.63	80.53	51.15	41.65	20.5
225°C-30min	90.15	140.8	4.03	0.87	76.37	53.67	39.02	21.11
225°C-45min	74.15	126.4	3.95	0.94	65.45	58.63	34.70	22.50
250°C-15min	90.71	145.6	4.13	1.00	76.57	53.02	39.28	21.28
250°C-30min	78.21	128.4	6.68	0.96	70.03	57.14	35.83	22.40
250°C-45min	66.32	114.3	4.20	1.08	59.75	62.26	31.16	24.01
275°C-15min	80.66	123.1	4.15	0.94	70.90	56.59	36.28	21.91
275°C-30min	61.47	113.8	4.18	0.98	56.53	64.17	29.27	24.72
275°C-45min	46.67	102.6	5.02	1.40	43.17	71.48	22.81	26.68

3.3.2. Component analysis

Extractives, structural carbohydrates and lignin in control and torrefied pine were analyzed using Laboratory Analytical Procedure (LAP) developed by the National Renewable Energy Laboratory [27]. The fraction of biomass components obtained was normalized by mass loss during torrefaction to get the values as a percentage of original non-torrefied biomass (Eq. 1 and 2). If one of the biomass components (for example, hemicellulose) has been affected by torrefaction, then the fraction of other two components will automatically increase. Normalizing the fraction by mass loss puts into evidence the actual loss of each component induced by torrefaction.

$$Mass\ loss\ during\ torrefaction,\ \Delta m = (m_i - m_f)/m_i \quad \text{(Eq. 1)}$$

$$Normalized\ wt.\%\ of\ each\ component\ =\ wt.\%\ obtained\ for\ torrefied\ samples \times (1 - \Delta m) \quad \text{(Eq. 2)}$$

where, m_i = initial mass of biomass before torrefaction (g)

m_f = final mass of torrefied biomass (g)

3.3.3. CP MAS ^{13}C NMR

The solid-state CP/MAS ^{13}C NMR was performed on a Bruker Avance III 400 MHz spectrometer operating at frequencies of 100.59 MHz for ^{13}C. A Bruker double-resonance 4-mm MAS probe head was used and the experiments were carried out at ambient temperature. The samples were packed in a 4 mm ZrO rotor fitted with a Kel-F cap. The CP/MAS ^{13}C spectra were acquired with a CP pulse sequence and 3072 scans were accumulated for each sample. For quantitative analysis, area under the curve obtained by integrating the NMR spectra at different ppm was normalized by mass used in the rotor and mass lost during torrefaction as shown in Eq. 3 [17].

$$Normalized\ area = \frac{Actual\ area}{m} \times (1 - \Delta m) \quad \text{(Eq. 3)}$$

where, m is mass of sample used in rotor and Δm is calculated according to Eq. 1.

3.3.4. XRD

Cellulose crystallinity in control and torrefied samples was measured using Bruker D2 Phaser X-ray diffractometer (XRD). The instrument scanned 2θ from 10 to 40^{o}. Time for each scan was 0.5 s and data was recorded at every 0.01415^{o}. Crystallinity index (CrI) of cellulose in the samples was calculated according to the Eq. 4 [28] after subtraction of the background.

$$CrI = \frac{I_{002} - I_{am}}{I_{002}} \times 100\ \% \qquad \text{(Eq. 4)}$$

where, I_{002} (at 2θ = ~22 ^{o}) is the maximum peak intensity and I_{am} (at 2θ = ~18 ^{o}) is the minimum intensity between peaks at 2θ = ~15.5 ^{o} and ~22 ^{o}.

3.3.5. Py-GCMS

Pyrolysis of the samples was performed in triplicates and in random order using a commercial pyrolyzer (Pyroprobe model 5200, CDS Analytical Inc., Oxford, PA) coupled with a GC-MS (Agilent 7890 GC/5975 MS) and equipped with a DB 1701 column for products separation. Approximately 2-3 mg of sample (particle size 0.297mm – 0.420 mm) was packed between quartz wool in a quartz tube (25 mm long and 1.9 mm internal diameter) and placed in the pyrolysis chamber. The pyrolysis experiments were carried out at 550 °C (filament temperature) with heating rate of 2000 °C/s and held for 90 s at final temperature. The interface temperature was kept at 300 °C and purged with helium flowing at rate of 20 mL/min. When the pyrolysis starts, condensable gases were transferred to trap, where they are absorbed at 40 °C, and later desorbed at 300 °C and carried to GC column. The transfer line and the injector were kept at 300 °C and 250 °C respectively. The chromatograph oven was ramped from 45 °C (hold time =

5min) to 240 °C (hold time = 8min) at a rate of 5 °C/min. Mass spectrometer was operated by the electron impact ionization mode at 69.9 eV and mass scan range was 50-550 Da. Compounds were identified using the National Institute of Standards and Technology (NIST) mass spectral library. Compounds appearing consistently and with high quality were selected and quantified. Quantification was done by injecting calibration standards, which were prepared by dissolving approximately 100 mg of each compound in 100 mL of dichloromethane and diluting them to different concentrations with methanol. Standards were injected three times and average area was taken for calibration. The slope of calibration line obtained by plotting concentration of compound versus its area was taken as the quantification factor in the calculation. For all the experiments, split ratio was set to 50:1 and helium flowing at 0.763 mL/min was used as carrier gas. Percentage carbon yield from each compound was calculated using Eq. 5 [29].

$$\%\ carbon\ yield = \frac{mass\ of\ compound \times mass\ fraction\ of\ carbon\ in\ each\ compound}{mass\ of\ biomass \times mass\ fraction\ of\ carbon\ in\ biomass} \times 100 \qquad \text{(Eq. 5)}$$

ZSM-5 (SiO_2/Al_2O_3 = 30, surface area = 425 m^2/g) catalyst used in catalytic pyrolysis experiments was purchased from Zeolyst, Inc. and received in ammonium cation form. It was calcined in air at 550 ^oC for 2 h in a furnace for conversion into H^+ZSM prior to use. Biomass samples were mixed with the catalyst in ratio of 1:9 for all catalytic experiments.

3.3.6. Statistical analysis

Statistical analyses were performed using SAS 9.2 (Cary, NC). Analysis of variance (ANOVA) was performed to evaluate the effect of torrefaction temperature and time on the results of component analysis and product yield from pyrolysis. Linear regression was performed to

evaluate the relationship between biomass structures and aromatic production. All analyses were performed at significance level, $\alpha = 0.05$.

3.4. Results

3.4.1. Component analysis

Table 3.3 shows total extractive, carbohydrates and lignin percentage in control and torrefied biomass after accounting for mass loss during torrefaction. Statistically, no difference was observed in the amount of extractive in the torrefied samples when compared to control, except for 275^{o}C-45min where it was significantly reduced. It is also apparent that hemicellulose was significantly degraded due to torrefaction, starting from sample 225^{o}C-30min where it was reduced by 29.6%. For samples torrefied at the two most severe conditions (275^{o}C-30min and 275^{o}C-45min), no hemicellulose peaks were observed showing that the biomass hemicelluloses completely degraded at these conditions. Significant reduction in cellulose wt.% was apparent only in samples torrefied at higher severity (225^{o}C-45min, 250^{o}C-30min, 250^{o}C-45min, 275^{o}C-15min 275^{o}C-30min and 275^{o}C-45min). Maximum cellulose degradation took place at 275^{o}C-45min, where it was reduced by 95.4%. Acid insoluble lignin (AIL), shown in Table 3.3 represents the total acid insoluble components in biomass (including ash and condensation products of cellulose and hemicellulose degradation). Sample torrefied at 225^{o}C-30min demonstrated a 23.4% reduction in AIL as compared to control sample. This initial reduction in lignin can be attributed to structural changes in lignin (demethoxylation and cleavage of ether linkages) as revealed by ^{13}C NMR spectra, which can cause initial mass loss of AIL. Significantly higher AIL% in samples torrefied at high severity (225^{o}C-45min, 250^{o}C-45min,

275°C-15min, 275°C-30min and 275°C-45min) might be due to the poly-condensation reactions between polysaccharides degradation products that forms "pseudo-lignin" during dilute acid pretreatment which leads to over estimation of AIL [15, 30].

Table 3.3 Component analysis (wt.%)

Sample	Cellulose % (Glucan)	Hemicellulose %					Lignin %		Extractive %
		Xylan	Galactan	Arabinan	Mannan	Total	AIL	ASL	
Control	39.08[a]	6.88	2.94	1.87	12.51	24.21[a]	30.29[d,e]	0.37[a]	2.99[a]
225°C-15min	41.15[a]	7.84	2.80	1.22	13.51	25.38[a]	29.49[e]	0.31[a,b,c]	2.48[a,b]
225°C-30min	39.73[a]	4.70	1.59	0.54	10.21	17.04[b]	23.20[f]	0.33[a,b,c]	3.11[a]
225°C-45min	27.89[c]	1.28	0.19	0.00	3.90	5.38[d]	38.27[b,c]	0.27[c,d]	1.92
250°C-15min	40.32[a]	5.41	1.77	0.66	11.03	18.87[b]	27.25[d,e]	0.20[d]	2.90[a]
250°C-30min	32.86[b]	1.07	nd	nd	3.82	4.89[d]	37.03[c,d]	0.34[a,b]	2.08[a,b]
250°C-45min	19.55[d]	0.27	nd	nd	1.29	1.57[e]	44.38[a,b]	0.31[a,b,c]	1.27[a,b]
275°C-15min	34.84[b]	2.54	0.43	0.21	5.93	9.11[c]	40.54[c]	0.34[a,b]	1.12[a,b]
275°C-30min	15.39[d]	nd	nd	nd	nd	nd	46.27[a]	0.29[b,c]	1.11[a,b]
275°C-45min	1.85[e]	nd	nd	nd	nd	nd	46.47[a]	0.10[e]	0.43[b]

Any two means in the same column with different letters are significantly different ($p<0.05$) by the Tukey's HSD test. The letters a-f in superscript refer to the highest estimates to the least. All values are calculated in dry basis. Cellulose, hemicellulose and lignin are calculated in extractive free basis. nd: not detected; AIL: acid insoluble lignin; ASL: acid soluble lignin.

3.4.2. CP MAS ^{13}C NMR

^{13}C NMR peaks assignment was done according to literature as listed in Table 3.4 and ^{13}C NMR peaks for samples are shown in Figure 3.1.

Table 3.4 Assignment of signal from CP/MAS ^{13}C NMR [17, 31-33]

Chemical shift (ppm)	Bond assignment
206	Ketone
173	Acetyl carboxyl (Hemicellulose)
152	Ether linked - Guaiacyl, C-3/4
148	Guaiacyl non-ether linked, C-3/4
110-140	Aromatic C-C and C-H
105	Cellulose/xylan C-1
89	Crystalline cellulose C-4
83	Amorphous cellulose C-4/ xylan
72 and 75	Cellulose C-2/3/5; xylan C-2/3
65	Crystalline cellulose C-6
62	Amorphous cellulose C-6/xylan C-5
56	Lignin methoxyl
32	Aliphatic
21	Acetyl methyl (hemicellulose)

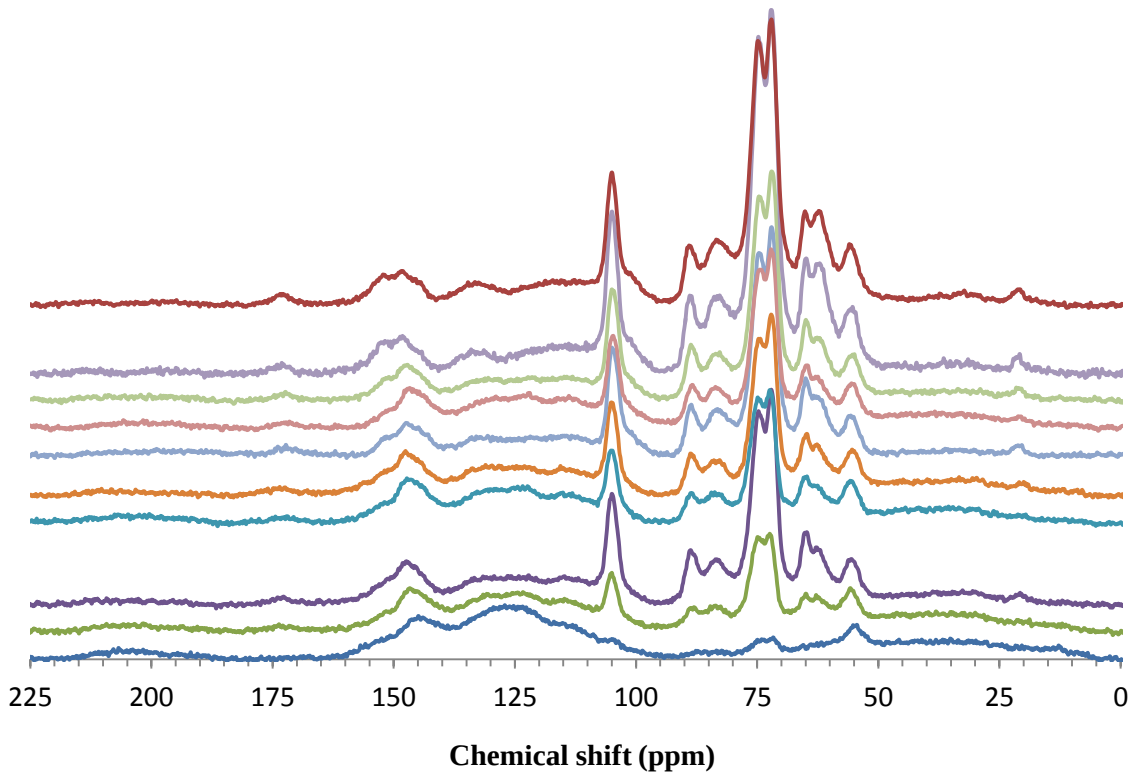

Figure 3.1 ^{13}C NMR Spectra of (from top to bottom): Control, 225^{o}C-15min, 225^{o}C-30min, 225^{o}C-45min, 225^{o}C-15min, 250^{o}C-30min, 250^{o}C-45min, 275^{o}C-15min, 275^{o}C-30min, 275^{o}C-45min

Peaks at 173 and 21 ppm, respectively are assigned to acetyl carboxyl and acetyl methyl groups of hemicellulose. Clear and distinct hemicellulose peaks can be seen for control sample. Acetyl carboxyl peak was present in all torrefied samples except the sample 275^{o}C-45min, where it completely disappeared. Acetyl methyl peak was absent in samples torrefied at the two most severe conditions (275^{o}C-30min and 275^{o}C-45min). The plot of normalized area of hemicellulose peaks at different torrefaction condition is shown in Figure 3.2 (a, b). Although component analysis (Table 3.3) indicated no significant reduction in hemicellulose sugars for sample treated at 225^{o}C-15min, results from NMR analysis revealed 46.9 and 20.9 % reduction

in its acetyl carboxyl and acetyl methyl components respectively. This implies that torrefaction caused deacetylation of hemicellulose even at mild condition of 225^{o}C-15min.

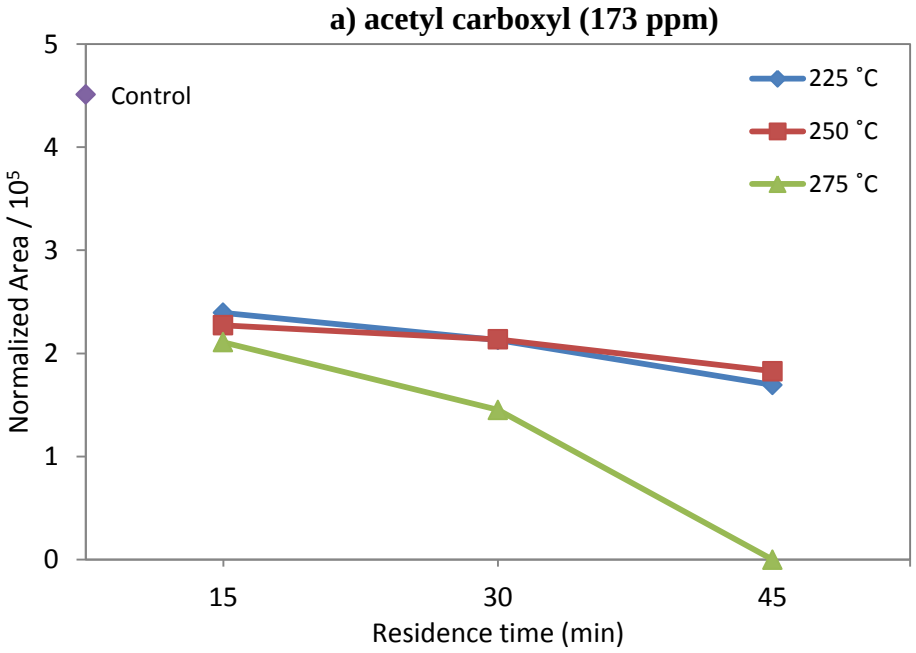

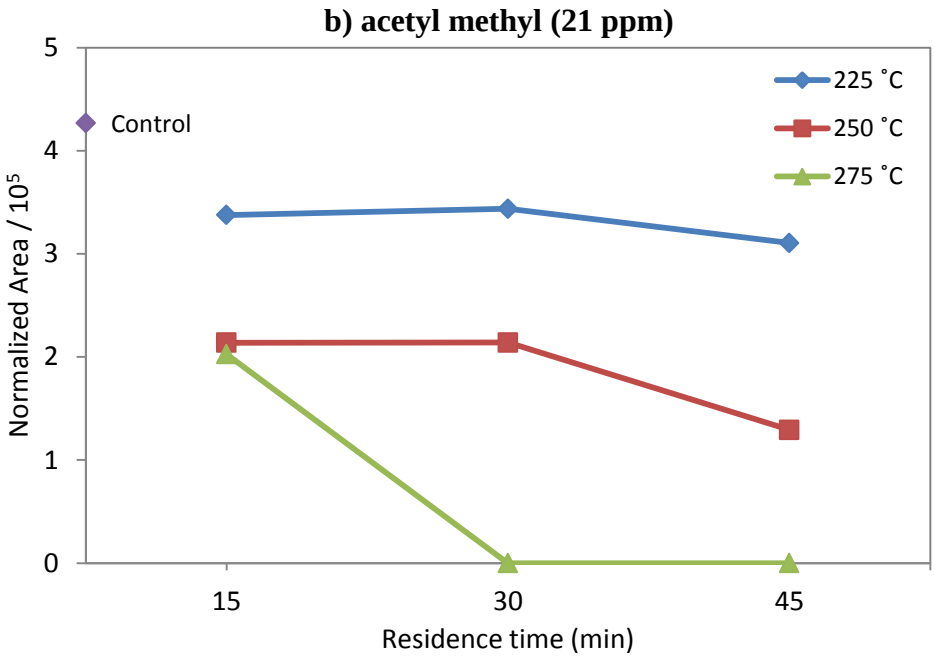

Figure 3.2 Normalized area of hemicellulose components at different torrefaction conditions a) Acetyl carboxyl b) Acetyl methyl

Large signals in interval 62-105 ppm are predominantly assigned to cellulose and to a lesser extent to hemicellulose carbohydrates. These signals were seen to have consistent pattern in all the samples except for 275^{o}C-45min, where most of these signals disintegrated showing that cellulose was mostly decomposed at this condition. This result is consistent with component analysis from which we obtained only 1.85% of cellulose in this sample. Normalized total area of cellulose peaks plotted against torrefaction conditions is shown in Figure 3.3, which shows that the total gylcosidic components increased slightly (10% as compared to control) at 225^{o}C-15min and then decreased markedly with increase in torrefaction severity. Dramatic reduction (28% as compared to control) in normalized total area of these signals for 225^{o}C-30min can be attributed to degradation of xylan of hemicellulose rather than cellulose, as these signals also contain overlapping signal of C1-C5 of xylan in hemicellulose.

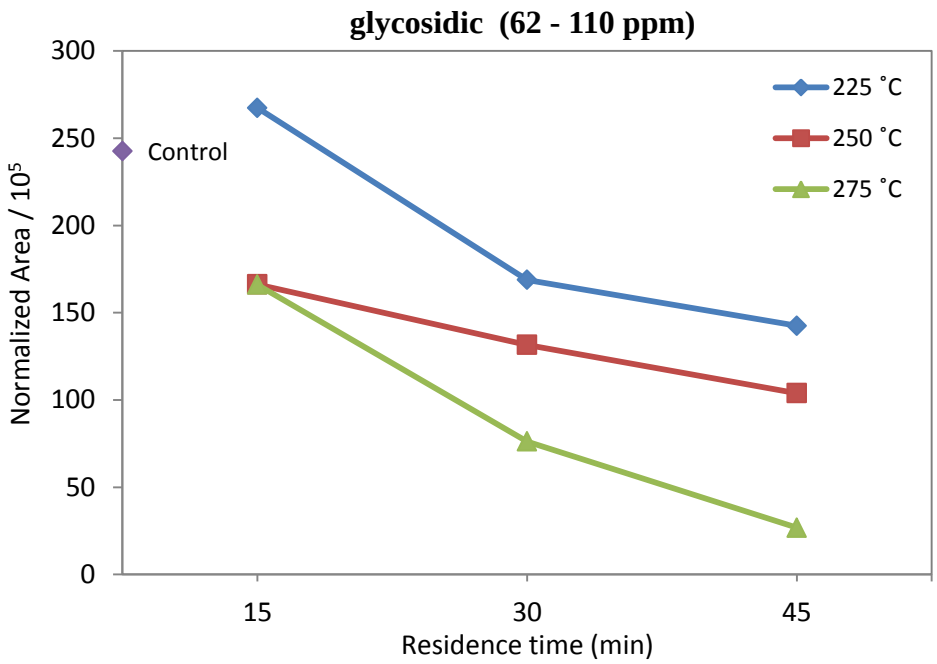

Figure 3.3 Normalized area of total glyosidic linkages at different torrefaction conditions

Among lignin peaks, major observation was made in the peaks at 152 and 148 ppm. These peaks are assigned to ether linked and non-ether linked guaiacyl lignin, respectively. For control sample, two distinct overlapping peaks were observed as shown in Figure 3.1. With torrefaction, it was observed that ether linked signal at 152 ppm gradually shifted and merged with non-ether peak at 148 ppm. Figure 3.4 (a, b, c) show the normalized peak area of lignin components (at 152, 148 and 56 ppm) at different torrefaction severity. Sharp decrease in ether linkages (50.16%) and lignin methoxyl (28.36%) groups when torrefaction severity was increased from 225^{o}C-15min to 225^{o}C-30min shows that these lignin components started to degrade at this torrefaction range. Decrease in ether linkage of lignin was more prominent when torrefaction time was increased from 15 to 30 min in all three temperatures as shown in Figure 3.4 (a). Increase in non-etherified C-3/5 components as shown in Figure 3.4 (b) imply that during torrefaction ether linkages cleaved to form non-ether linked guaiacyl components. Lignin

methoxyl components (Figure 3.4 (c)), which are directly linked to methoxy carbon in guaiacyl unit, is observed to decrease with torrefaction residence time at 225 ^{o}C and 275 ^{o}C. However, a slight increase was observed at 250 ^{o}C, when torrefaction time was increased from 15 to 30 min.

a) ether linkage (152 ppm)

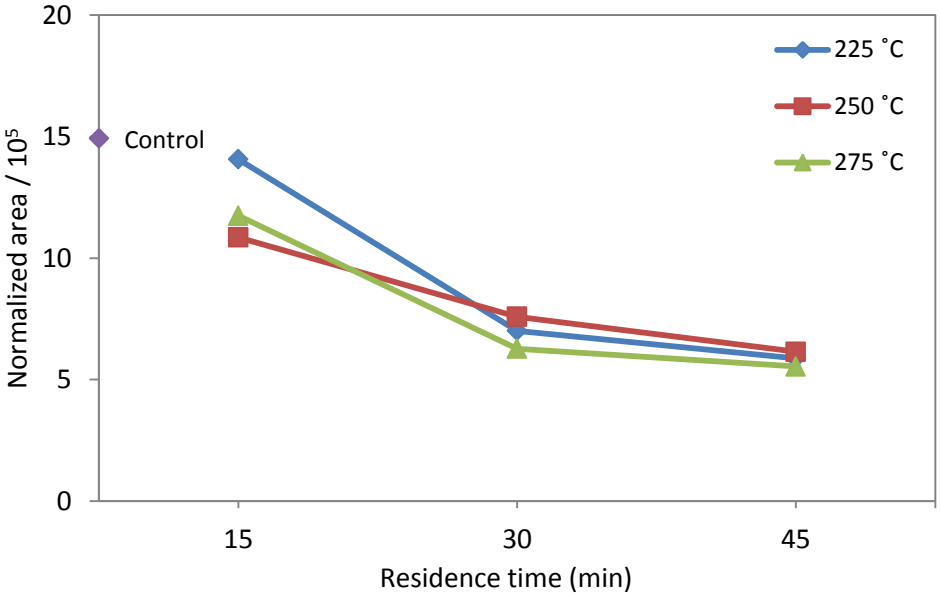

b) non-ether linkage (148 ppm)

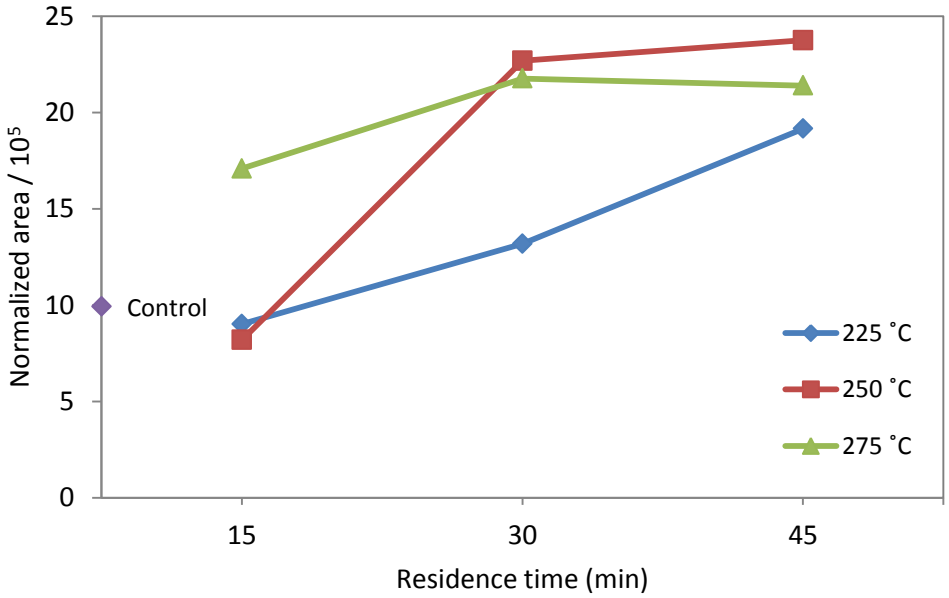

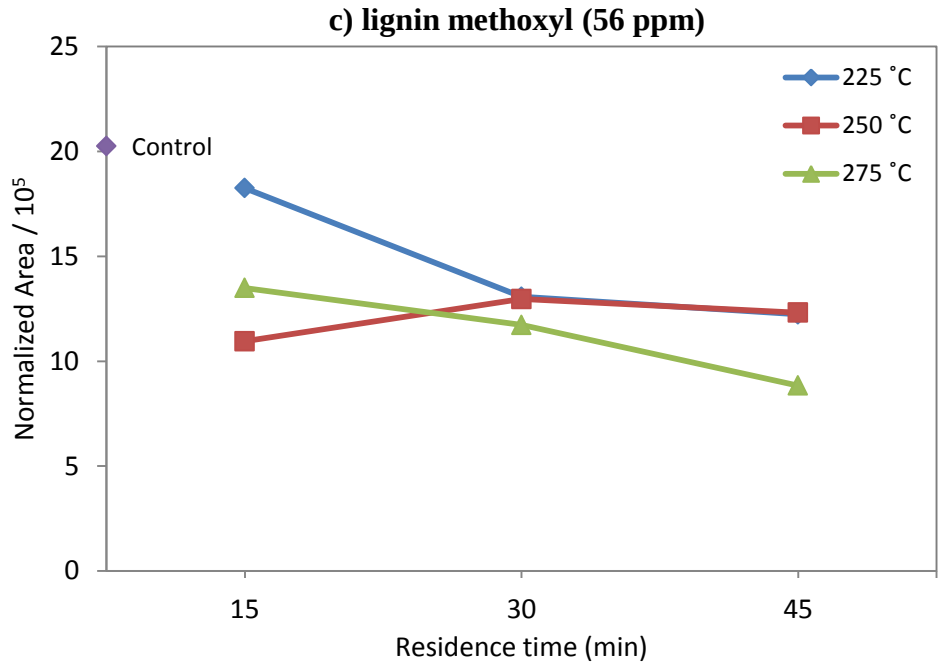

Figure 3.4 Normalized area of lignin components at different torrefaction conditions a) Ether linked b) Non-ether linked c) Lignin methoxyl

The weakening of hemicellulose and cellulose signals in NMR spectra of torrefied samples was accompanied by overall broadening of aromatic (110-140 ppm) and aliphatic (centered at 32 ppm) signals, the normalized plot of which are shown in Figure 3.5 (a, b). It is also evident that intensity of aromatic signals first decreased (by 2.3, 6.1 and 18.3 % for samples 225^{o}C-15min, 225^{o}C-30min and 250^{o}C-15min, respectively), and then increased at more severe torrefaction conditions. Similarly, aliphatic signals also decreased initially (by 12.6, 6.3 and 55.8% for samples 225^{o}C-15min, 225^{o}C-30min and 250^{o}C-15min, respectively) before increasing at higher torrefaction severity. This indicates that aromatic and aliphatic components are first degraded by torrefaction at mild conditions. It should be noted that the same samples which encountered increase in aromatic and aliphatic signals also suffered significant cellulose degradation (from component analysis – Table 3.3). This implies that during torrefaction, cellulose degradation is accompanied by polymerization and recondensation reactions of primary decomposition

products to form aromatic and aliphatic C-C and C-H bonds [16, 32]. Few studies [16, 34, 35] have also proposed that cleavage of lignin ether bond can also re-condense to form aromatic C-C bonds. However, this couldn't be confirmed from this study as de-etherification of lignin was observed even at mild torrefaction conditions (225^{o}C-30min and 250^{o}C-15min), but increase in aromatic and aliphatic components did not occur until 225^{o}C-45min and 250^{o}C-30min. Broad resonance of ketone groups at about 206 ppm was also observed for samples torrefied at higher severity (225^{o}C-45min, 250^{o}C-45min, 275^{o}C-30min, 275^{o}C-45min), which implies that during torrefaction carbohydrate groups might have reacted to form ketone groups.

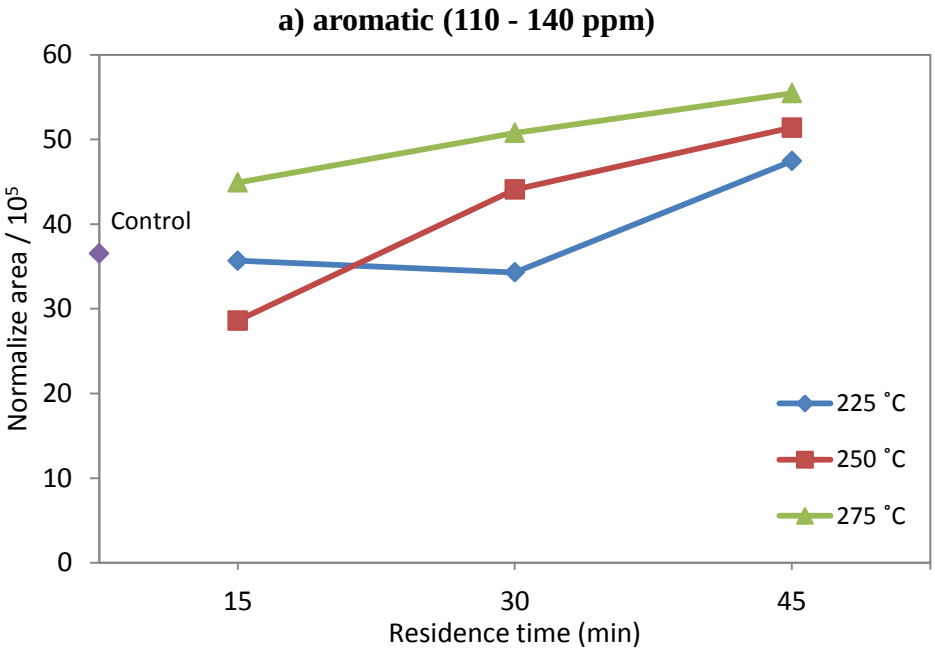

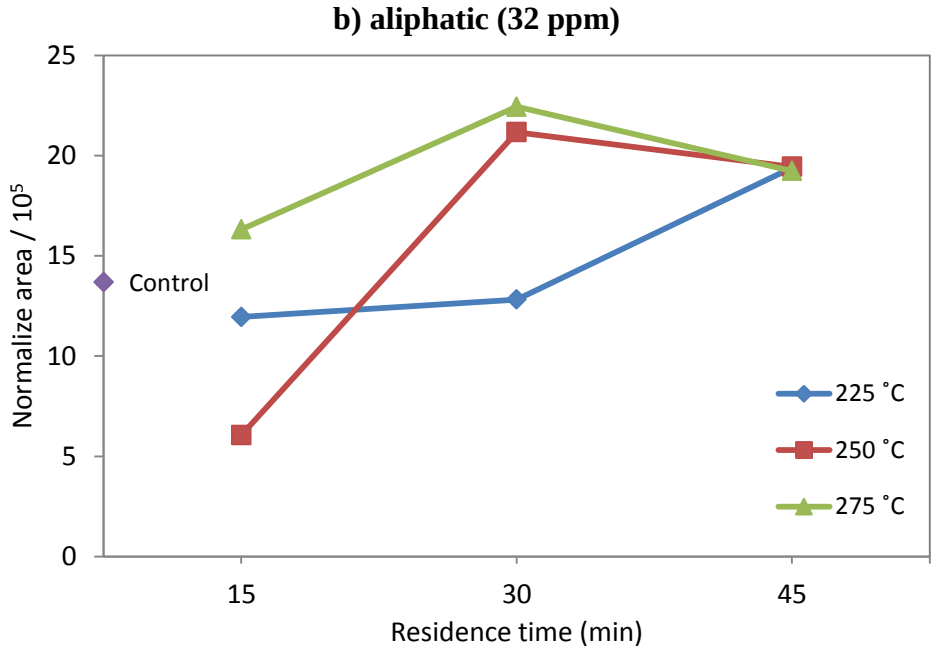

Figure 3.5 Normalized areas of a) Aromatic and b) Aliphatic signals at different torrefaction condition

Note: The point labeled control represents value for non-torrefied sample.

3.4.3. XRD

XRD spectra of untreated and torrefied pine samples are shown in Figure 3.6 and CrI of samples are listed in Table 3.5. CrI of pine torrefied at 225^{o}C-15 min was slightly higher (75.4%) than control pine. Further increase in torrefaction time and temperature resulted in decrease in CrI. As seen in Figure 3.6, XRD spectra for all the samples were similar showing two distinct peaks at 2θ ~ 16 ^{o} and 22 ^{o}, except for 275^{o}C-45min where peak at 2θ = 16^{o} completely disappeared. This is due to almost complete decomposition of cellulose at this condition as confirmed by results of component and NMR analysis. The initial increase in CrI suggested that amorphous cellulose partly recrystallized due to torrefaction before being degraded at higher temperature [15]. Apart

of XRD peak height method used in this study, XRD peak deconvolution and amorphous subtraction methods and ^{13}C NMR spectra have also been used to estimate CrI [36]. Sannigrahi et al. reported 63% CrI of untreated loblolly pine using ^{13}C NMR spectra [37]. The peak height method based on XRD pattern is mostly used to compare the relative CrI among different samples and produces significantly higher value than other methods [36].

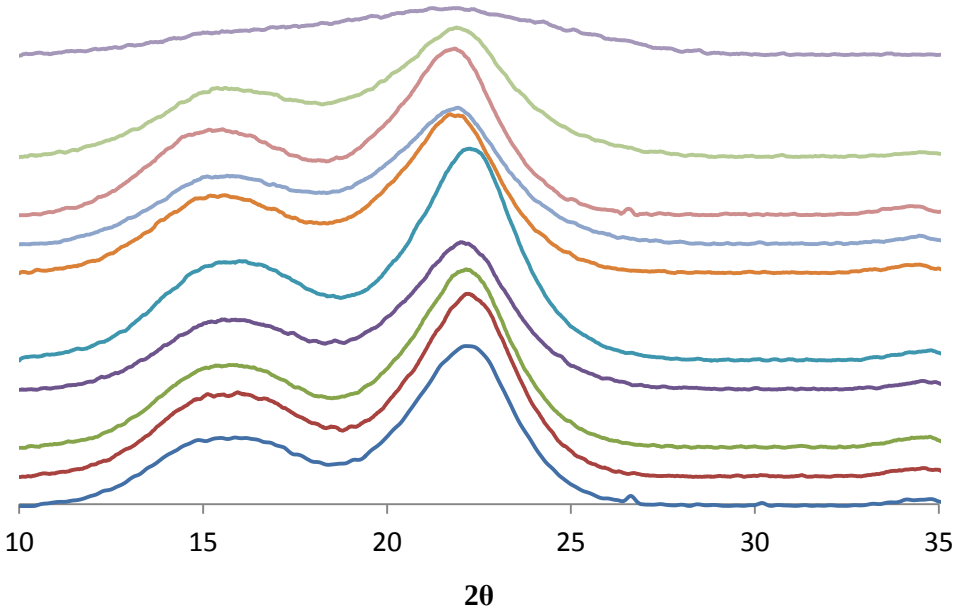

Figure 3.6 XRD spectra (from bottom to top): Control, 225°C-15min, 225°C-30min, 225°C-45min, 225°C-15min, 250°C-30min, 250°C-45min, 275°C-15min, 275°C-30min, 275°C-45min

Table 3.5 CrI of control and torrefied samples

Sample	CrI	2 θ	
		I_{002}	I_{am}
Control	75.03	22.14	18.41
225°C-15min	75.45	22.22	18.79
225°C-30min	72.92	22.14	18.51
225°C-45min	69.59	22.02	18.30
250°C-15min	71.00	22.22	18.75
250°C-30min	69.43	21.71	18.22
250°C-45min	63.35	21.93	18.37
275°C-15min	68.47	21.85	18.35
275°C-30min	60.14	21.90	18.27
275°C-45min	-	-	-

3.4.4. Py-GC/MS: Non-catalytic pyrolysis

More than 300 compounds were detected from MS library. For each run, approximately 100 compounds with major peak areas were chosen and integrated. Among them, 38 compounds with high quality and occurring consistently in all the runs were selected for quantification. These compounds were grouped into five categories: aromatic hydrocarbons, phenolic, guaiacol, furan and ketone, depending on their functional groups. The compounds quantified under each group are listed in Table 3.6.

Table 3.6 List of compounds quantified for non-catalytic pyrolysis

Aromatic	Phenolic	Guaiacol	Furan	Ketone
Benzene	Phenol	Phenol, 2-methoxy-	Furan, 2-methyl-	2-Cyclopenten-1-one, 2-methyl
Toluene	Phenol, 2-methyl-	Phenol, 2-methoxy-4-methyl	Furan, 2,5-dimethyl-	2-Cyclopenten-1-one, 3-methyl
Ethylbenzene	Phenol, 2,3-dimethyl-	Phenol, 4-ethyl-2-methoxy	Furfural	2-Cyclopenten-1-one, 2,3 - dimethyl-
P-xylene	Phenol, 4-methyl	2-Methoxy-4-vinylphenol	Furan, 2-ethyl-5-methyl-	
o-xylene	Phenol, 2,4-dimethyl-	Eugenol	2-Furancarboxaldehyde, 5-methyl	
Styrene	Phenol, 2,3,6-trimethyl-	Phenol, 2-methoxy-4-(1-propenyl)-	2 (5H) - Furanone	
Benzene, 1,3,5-trimethyl	Phenol,3,5-dimethyl-	Phenol, 2-methoxy-4-(1-propenyl)-(Z)-		
Benzene, 1-ethyl-3-methyl	Phenol, 4-ethyl	Vanillin		
Benzene, 1,2,3-trimethyl	Phenol, 3,4-dimethyl	Ethanone, 1-(4-hydroxy-3methoxyphenyl)-		
Naphthalene	Phenol, 4-ethyl-3-methyl-			

Table 3.7 Carbon yield % from non-catalytic pyrolysis

Sample	Carbon yield %					Total
	Aromatic	Furan	Phenolic	Guaiacol	Ketone	
Control	0.13^{c}	3.07^{a}	0.99^{b}	$2.34^{a,b,c}$	$0.24^{a,b,c}$	$6.78^{a,b,c}$
225°C-15min	0.13^{c}	2.88^{a}	1.44^{b}	$1.95^{a,b.c}$	$0.45^{a,b}$	$6.85^{a,b,c}$
225°C-30min	0.15^{c}	$2.36^{a,b,c}$	2.64^{a}	$2.43^{a,b,c}$	$0.33^{a,b}$	$7.91^{a,b}$
225°C-45min	0.18^{c}	$1.59^{b,c,d}$	2.57^{a}	$1.47^{b.c}$	$0.17^{b,c}$	$5.99^{b,c}$
250°C-15min	0.18^{c}	$2.73^{a,b}$	2.67^{a}	$2.74^{a,b}$	$0.34^{a,b}$	$8.66^{a,b}$
250°C-30min	$0.20^{a,b,c}$	$2.00^{a,b,c,d}$	3.26^{a}	$2.66^{a,b,c}$	$0.21^{a,b,c}$	$8.32^{a,b}$
250°C-45min	$0.20^{a,b,c}$	$1.47^{c,d}$	3.16^{a}	$2.03^{a,b,c}$	$0.21^{a,b,c}$	$7.08^{a,b,c}$
275°C-15min	$0.19^{b,c}$	2.83^{a}	3.22^{a}	3.46^{a}	$0.09^{b,c}$	9.79^{a}
275°C-30min	0.32^{a}	$1.16^{d,e}$	3.45^{a}	$2.25^{a,b,c}$	0.05^{c}	$7.24^{a,b,c}$
275°C-45min	$0.32^{a,b}$	0.14^{e}	2.94^{a}	0.72^{c}	0.04^{c}	4.16^{c}

Any two means in the same column with different letters are significantly different ($p<0.05$) by the Tukey's HSD test. The letters a-f in superscript refer to the highest estimates to the least.

Table 3.7 shows the total carbon yield from these groups of compounds in control and torrefied samples as a percentage of total carbon present in the sample. The aromatic carbon yields from sample torrefied at two most severe conditions (275^{o}C-30min and 275^{o}C-45min) were significantly higher than control sample. Significant increase in selectivity (measured as ratio of carbon yield from particular group of compounds to the total carbon yield times 100) of aromatic compounds with torrefaction time was observed for sample torrefied at 275^{o}C (Figure 3.7 (a)). On the other hand, the selectivity of furan compounds (Figure 3.7 (b)), which are derived from hemicellulose decreased with torrefaction. Except for sample 225^{o}C-15min, torrefaction increased the yield of phenolic compounds to statistically similar level as shown in Table 3.7. Selectivity of phenolic compounds was observed to increase with torrefaction as shown in Figure 3.7 (c), reaching 70% for sample 275^{o}C-45min. Due to high standard deviations in the yield of ketone and guaiacol compounds, no significance difference as compared to control was observed in their yield from torrefied samples. ANOVA results also revealed that torrefaction temperature did not have significant effect on yield of guaiacol compounds. Variations in selectivity of guaiacol and ketone compounds with torrefaction condition are shown in Figures 3.7 (d, e).

a) aromatic selectivity

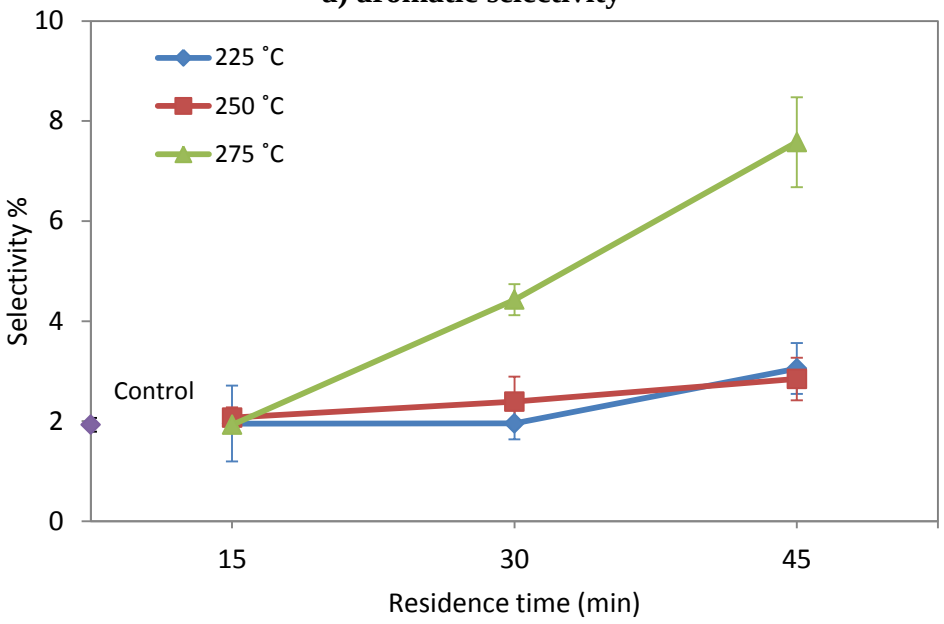

b) furan selectivity

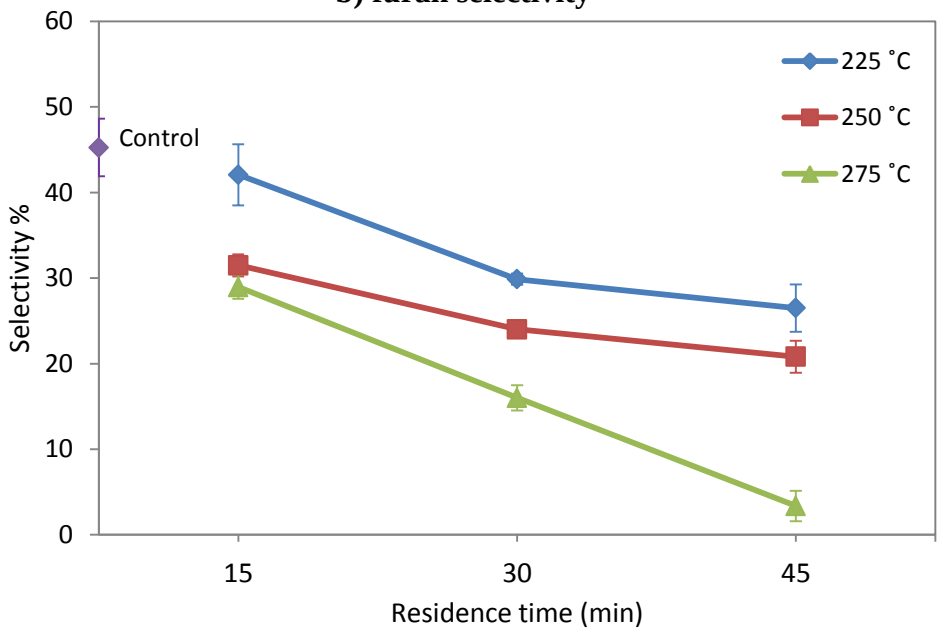

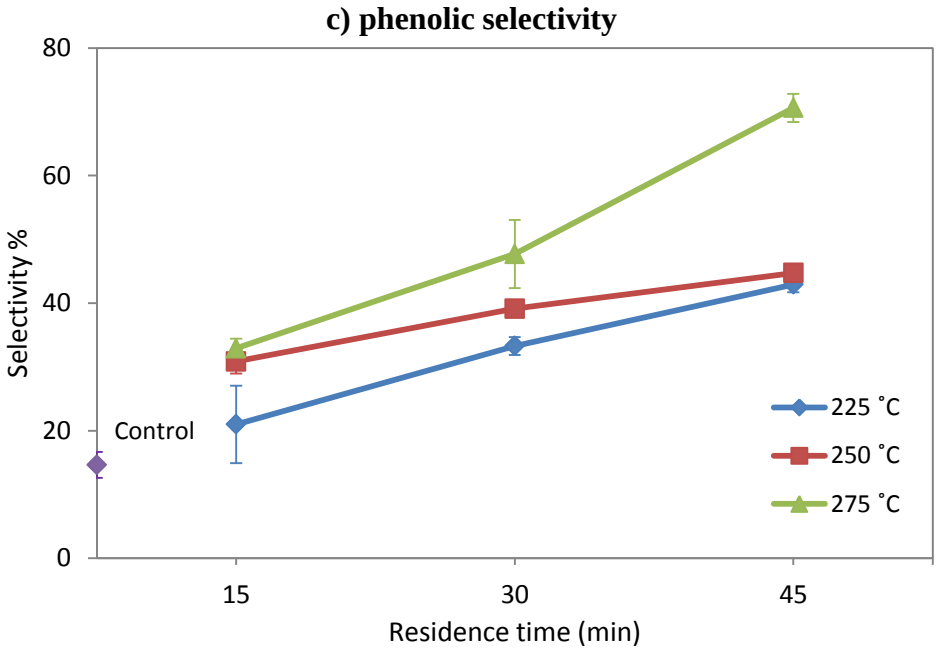
c) phenolic selectivity
80
60
40
20
0
Selectivity %
Control
225 ˚C
250 ˚C
275 ˚C
15
30
45
Residence time (min)

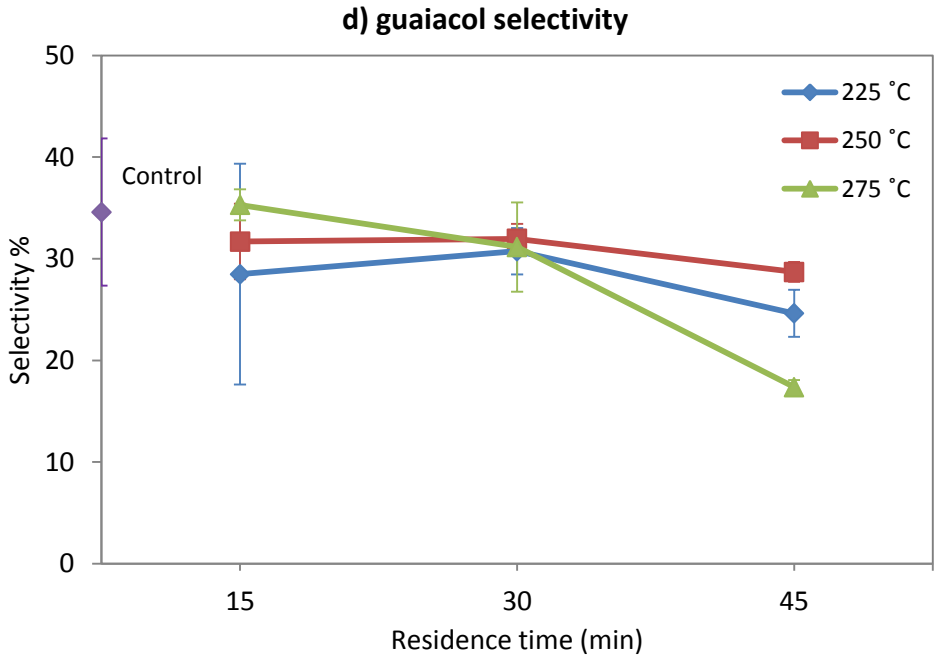
d) guaiacol selectivity
50
40
30
20
10
0
Selectivity %
Control
225 ˚C
250 ˚C
275 ˚C
15
30
45
Residence time (min)

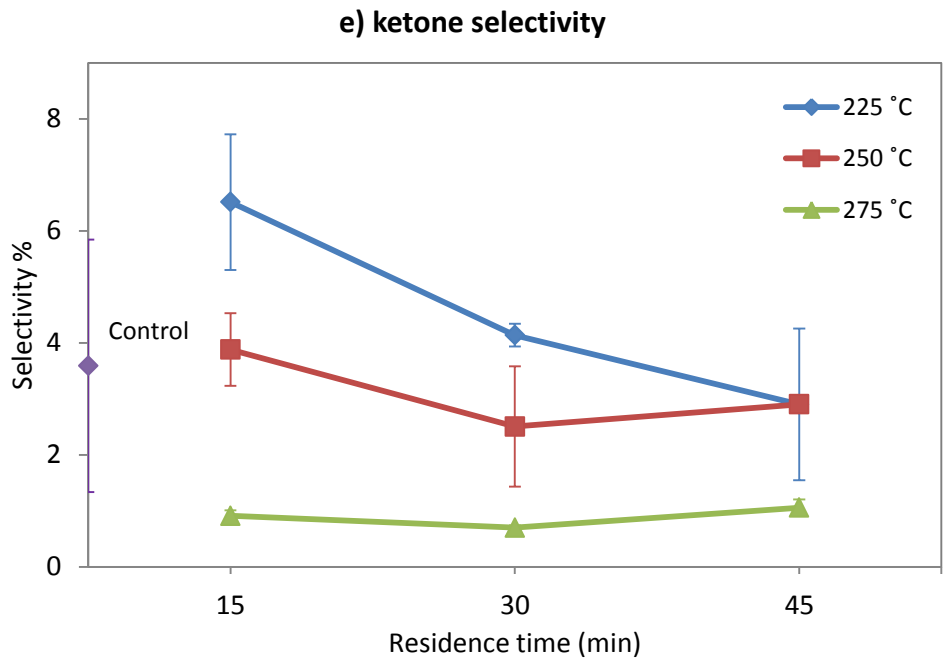

Figure 3.7 Selectivity of different compounds with torrefaction severity for non-catalytic pyrolysis

3.4.5. Py-GC/MS: Catalytic pyrolysis

Products from catalytic pyrolysis of both raw and torrefied pine were mostly aromatic and poly-aromatic hydrocarbons which included BTX compounds, benzene derivatives, naphthalenes, anthracene, phenanthrene and fluorene. Different group of compounds quantified is shown in Table 3.8. The carbon yield from different group of compounds is given in Table 3.9. Similar trend was observed for both aromatic and poly aromatic HC yield with change in torrefaction temperature and residence time. Total aromatic carbon yield for control sample was 22.8%. Maximum carbon yield from aromatics was obtained from torrefied samples at 225^{o}C-30min and 250^{o}C-15min, which was 38.2% and 37.3%, respectively. Using Tukey's multiple comparisons,

these values significantly differed from control sample but not within themselves. Also, pine torrefied at the most severe condition (275^{o}C-45 min) had the lowest aromatic yield (8.57%) which significantly differed from control and other torrefied samples. ANOVA analysis showed that torrefaction temperature, time and their interaction have significant effect on total aromatic yield from catalytic fast pyrolysis. Thus, it can be concluded that torrefaction affects aromatic production from catalytic fast pyrolysis using H^{+}ZSM-5 catalyst and torrefaction parameters – temperature and residence time play an important role in maximizing the aromatic yield. Yield of total oxygenated compounds, which included benzofurans, guaiacol and phenolic compounds were very less and varied from 0.02% (in 275^{o}C-45min) to 0.8% (in 225^{o}C-30min). Torrefaction parameters had no significant effect on yield of phenolic compounds. Similarly, no significance difference was found in yield of other oxygenated compounds (guaiacol and benzofuran) except from sample torrefied at most severe condition (275^{o}C-45min) where the yield of oxygenates was markedly lower.

Table 3.8 List of compounds quantified for catalytic pyrolysis

Aromatic	Poly-aromatic	Phenolic	Oxygenates (benzofurans and guaiacol)
Benzene	Naphthalene	Phenol	Benzofuran, 2-methyl
Toluene	Naphthalene, 1-methyl-	Phenol, 2-methyl-	Phenol, 2-methoxy-4-methyl
Ethylbenzene	Naphthalene, 2-ethyl-	Phenol, dimethyl	Dibenzofuran
p-Xylene	Naphthalene, 2,7-dimethyl-		
o-Xylene	Naphthalene, trimethyl		
Styrene	Fluorene		
Benzene, 1-ethyl-2-methyl-; Benzene, 1-ethyl-3-methyl	Fluorene, 1-methyl-		
Benzene, trimethyl-	Phenanthrene		
Benzene, 1-ethenyl-2-methyl- (Alpha methyl styrene); Benzene, 1-ethenyl-3-methyl-	Anthracene		
2,3 Benzofuran	Anthracene, 9-methyl-		
Indane	Phenanthrene, 2-methyl		
Indene			
Benzene, tetramethyl			
2-Methylindene			
Biphenyl			

Table 3.9 Carbon yield% from catalytic fast pyrolysis of raw and torrefied samples

Sample	Aromatics				Total aromatic HC	Oxygenates (benzofurans and guaiacol)	Phenolic
	BTX	Benzene derivatives	Naphthalene	Anthracene, phenanthrene and fluorene			
Control	10.56	5.9	5.85	0.55	$22.86^{b,c}$	$0.13^{a,b}$	0.08^{a}
225°C-15min	14.44	2.94	8.62	1.06	$27.05^{a,b,c}$	$0.16^{a,b}$	0.17^{a}
225°C-30 min	17.82	9.46	9.9	1.07	38.25^{a}	0.22^{a}	0.26^{a}
225°C-45min	13.13	5.75	6.91	0.89	$26.68^{a,b,c}$	$0.14^{a,b}$	0.28^{a}
250°C-15min	16.97	8.48	10.39	1.5	37.34^{a}	0.3^{a}	0.43^{a}
250°C-30min	16.33	8.53	9.15	1.5	$35.51^{a,b}$	$0.26^{a,b}$	0.61^{a}
250°C-45min	11.65	4.55	5.24	0.61	22.05^{c}	$0.05^{a,b}$	0.14^{a}
275°C-15min	15.72	5.4	7.67	1.02	$29.81^{a,b,c}$	$0.14^{a,b}$	0.3^{a}
275°C-30min	9.61	4.18	4.85	0.66	$19.3^{c,d}$	$0.05^{a,b}$	0.21^{a}
275°C-45min	4.3	1.84	2.14	0.29	8.57^{d}	0.00^{b}	0.04^{a}

Any two means in the same column with different letters are significantly different ($p<0.05$) by the Tukey's HSD test. The letters a-f in superscript refer to the highest estimates to the least.

3.5. Discussion

The differences in cellulose, hemicellulose and lignin in torrefied samples as compared to control are summarized in Table 3.10. In this section, we are interested in knowing the relationship between carbon yields and actual biomass structures (rather than changes due to torrefaction), so the values in the table have not been normalized by mass loss during torrefaction. They represent actual difference in amount cellulose, hemicellulose and lignin as compared to control sample. The not-normalized wt.% of cellulose, hemicellulose and lignin and ^{13}C NMR area of control and torrefied samples is given in Appendix A.

Table 3.10 Overall summary of effect of torrefaction on biomass components (as compared to control sample)

Sample	Difference hemicellulose			Difference in cellulose			Difference in lignin				Aromatic Components	Aliphatic Components
	wt %	Acetyl methyl	Acetyl carboxyl	wt %	Glycosidic components	CrI	AIL wt%	Ether linkage	Non-ether linkage	Lignin methoxyl		
225°C-15min	7.04	-50.17	-46.92	7.49	3.51	0.56	-0.61	-6.38	-7.80	-15.39	-8.32	-17.99
225°C-30min	-21.18	-47.66	-51.67	13.85	-22.85	-2.81	-17.37	-33.69	13.93	-28.44	4.09	3.86
225°C-45min	-70.07	-59.70	-60.13	-3.75	-36.93	-7.26	70.34	-54.24	4.81	-35.21	39.35	52.09
250°C-15min	-14.11	-46.60	-49.32	13.74	-27.34	-5.38	-0.73	-23.53	-25.24	-42.70	-13.49	-53.12
250°C-30min	-74.21	-47.72	-50.49	7.49	-40.11	-7.46	56.26	-15.16	40.34	-29.34	33.19	70.87
250°C-45min	-90.29	-56.31	-55.65	-24.83	-53.79	-15.57	120.97	-25.91	62.99	-34.42	51.68	53.29
275°C-15min	-53.35	-51.11	-51.74	10.52	-28.41	-8.74	65.90	-16.95	41.92	-30.35	28.52	24.69
275°C-30min	-100.00	-60.87	-62.72	-36.04	-61.79	-19.85	148.69	-35.24	53.09	-29.64	68.87	99.32
275°C-45min	-100.00	-100.00	-100.00	-90.05	-84.16	-52.71	228.9	-55.98	56.42	-37.53	117.36	101.37

Note: Positive sign represents increase % and negative sign represents decrease % as compared to control sample.

Non-catalytic pyrolysis and biomass structure:

For non-catalytic pyrolysis, significantly high aromatic HC yield from 275°C-30min and 275°C-45min can be attributed to high amount of components with aromatic C-C bonds in these samples as a result of condensation of cellulose degradation products during torrefaction as shown by ^{13}C NMR results. Stepwise regression performed at $\alpha = 0.05$ showed that aromatic components in biomass were linearly related to aromatic HC yield with correlation of $R^2 = 0.77$ as shown in Figure 3.8. Degradation of cellulose and hemicellulose followed by subsequent poly-condensation reactions during torrefaction at 275°C-30min and 275°C-45min resulted in biomass which is rich in aromatic components. As a result, during fast pyrolysis, increased yield of aromatic HC was observed.

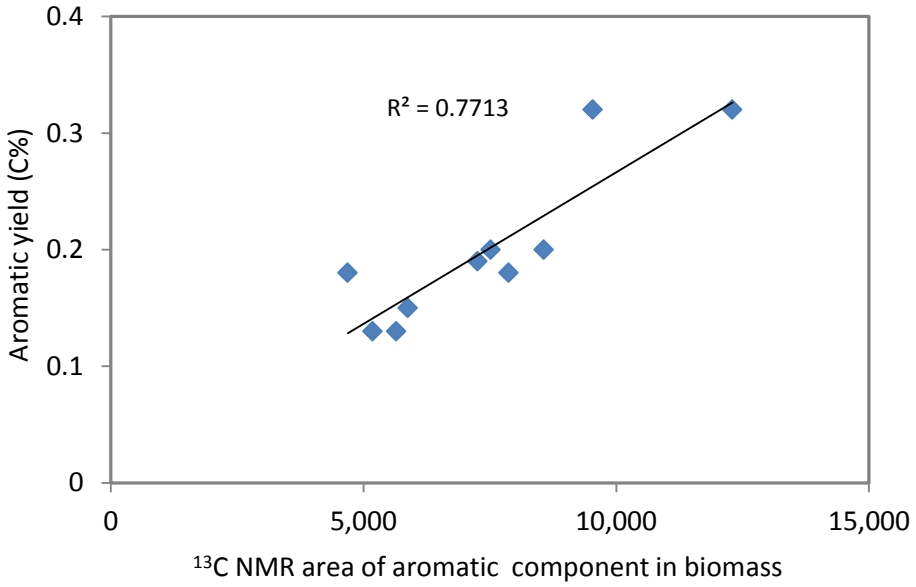

Figure 3.8 Plot of aromatic HC yield from non-catalytic pyrolysis versus aromatic components in biomass

The decrease in yield of furan compounds is due to reduction of hemicellulose components. The linear plot of wt.% of hemicellulose and furan yield is shown in Figure 3.9. R^2 value of 0.75 was

obtained and regression analysis showed that the parameter estimate for hemicellulose is significant at $\alpha = 0.05$.

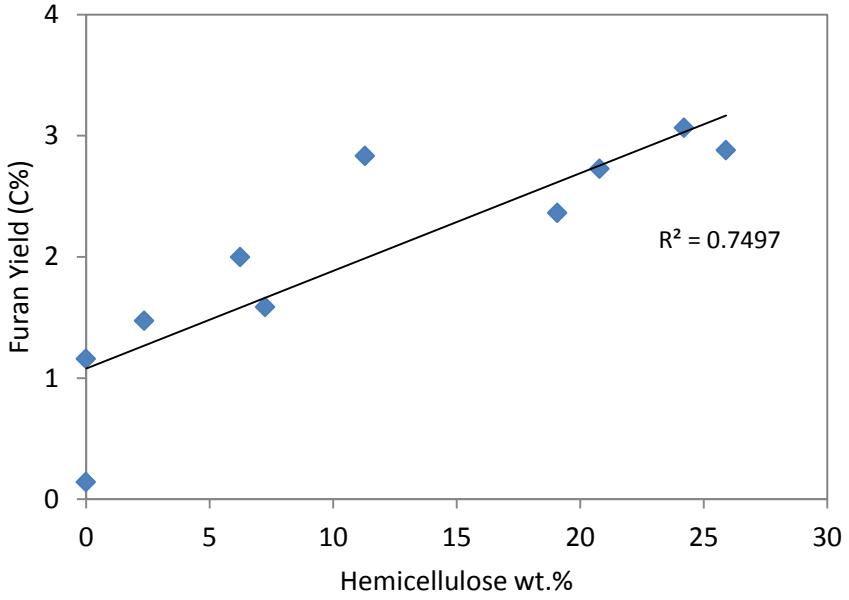

Figure 3.9 Yield of furan compounds versus wt.% of hemicellulose in biomass

Increase in phenolic yield due to torrefaction at 225°C-30min and higher can be attributed to changes in lignin structure characterized by cleavage of ether linkages and demethoxylation. Stepwise regression (at $\alpha = 0.05$) yielded the following equation (Eq. 6) for phenolic yield. The variable considered were lignin wt.%, non-ether and ether linkages in lignin and lignin methoxyl component. Only non-ether and methoxyl components were significant, the former having positive effect, while the latter having negative effect on the phenolic yield. This model accounts for 80% ($R^2 = 0.80$) of variation in the data set. The plot of predicted versus actual phenolic yield is shown in Figure 3.10.

$$Phenolic\ Yield = 4.52 + 2.97 \times 10^{-9}(non - ether) - 1.23 \times 10^{-8}(methoxyl) \qquad \text{(Eq .6)}$$

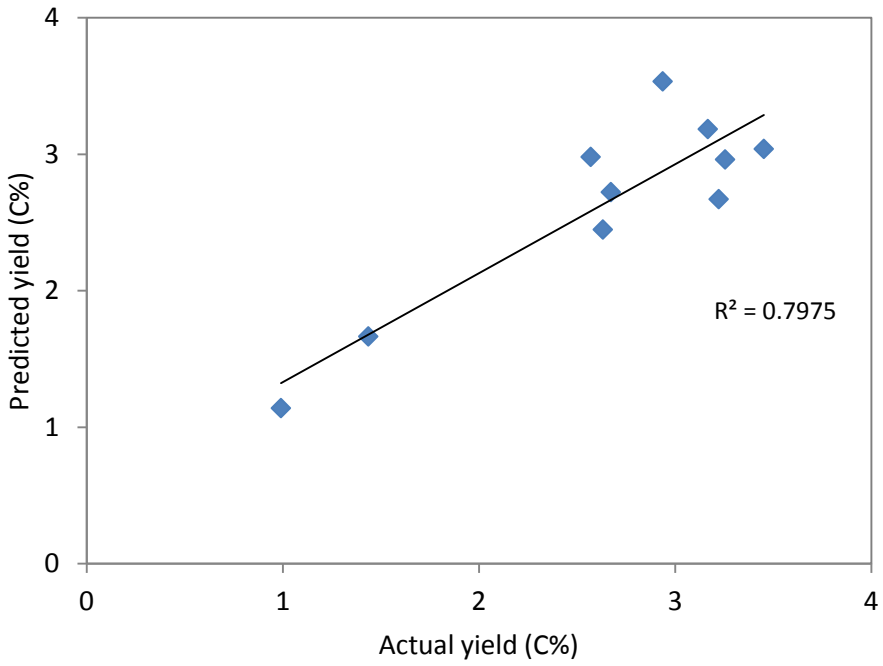

Figure 3.10 Predicted phenolic yield versus actual phenolic yield

Demethoxylation of guaiacyl lignin to form p-hydroxyphenyl units in torrefied biomass can favor production of phenolic compounds and reduce the guaiacols [38]. Torrefied biomass also contains higher lignin fraction which can increase lignin derived phenolic and guaiacol compounds. Increase in phenolic yield when torrefied lignin was used instead of raw lignin has also been reported in the previous study [10]. Pyrolysis of torrefied switchgrass has also shown increase in the phenolic compounds with increase in torrefaction temperature from 230 ^{o}C to 270 ^{o}C [39].

Significantly lower total carbon yield from 275$^{\mathbf{o}}$C-45 min is due to charring of cellulose caused by crosslinking and polycondensation reactions which can result in lower bio-oil yield and high char [40]. It is also noteworthy that total carbon yield from non-catalytic pyrolysis (ranging from 3.92 – 9.42%) in all the samples is very low as compared to that from catalytic pyrolysis (ranging from 8.6 -38.7%). This can be because compounds from catalytic pyrolysis contain

more of lower molecular weight volatile compounds like BTX which can easily be detected by GC-MS. Also, the boiling point of many phenolic products (especially high MW compounds from non-catalytic pyrolysis) are higher than the maximum temperature of the GC column (280 °C in the present study), and thus cannot be detected by MS despite their volatility [41]. In addition, in the present study the yield of levoglucosan, which can contribute to a major portion of total yield from non-catalytic pyrolysis, has not been quantified due to inconsistency in devolatization from pyroprobe.

Catalytic pyrolysis and biomass structure:

For catalytic pyrolysis, samples torrefied at 225^{o}C-30min and 250^{o}C-15min yielded maximum aromatic HC, which was 67.3 and 63.3% higher than catalytic pyrolysis of non-torrefied pine. One of the reasons for high aromatic production from these samples could be that at these torrefaction conditions, cellulose degradation had not started but there was significant reduction in wt.% of hemicellulose. Therefore, these samples actually contain comparatively higher fraction of cellulose (nearly 14% higher than control) as shown in Table 3.10. It has been reported in past studies that the rank order of aromatic yield among biomass components from catalytic fast pyrolysis using H^{+}ZSM-5 is cellulose > hemicellulose > lignin and that of polyaromatic is cellulose > lignin > hemicellulose [42, 43]. The reaction mechanism for conversion of cellulose into aromatics during catalytic fast pyrolysis involves thermal decomposition of cellulose to form anhydrosugars, primarily levoglucosan, which can undergo fragmentation and dehydration reactions to form furans and other small oxygenates. These oxygenates can diffuse into the channels of zeolite, where they undergo series of dehydration,

oligomerization, decarbonylation and decarboxylation reactions to form aromatics, olefins, CO_2, CO and water [44, 45]. Linear plot of fraction of cellulose and aromatic HC yield from catalytic fast pyrolysis is shown in Figure 3.11 (a). R^2 value of 0.81 was obtained and the parameter estimate for cellulose was also found to be significant at $\alpha = 0.05$.

Another reason for increase in aromatic and total carbon yield from samples 225^{o}C-30min and 250^{o}C-30min can be attributed to changes in structure of lignin. During catalytic fast pyrolysis of lignin, thermal decomposition of lignin takes place to form phenols, which diffuse into the pores of zeolite to form aromatics and olefins [44-46]. Non-catalytic pyrolysis of biomass torrefied at 225^{o}C-30min and higher have shown increased production of phenolic compounds (Table 3.7), which was attributed to cleavage of ether linkages and demethoxylation of lignin. Therefore, it can be implied that torrefied biomass results in increased production of phenolic compounds, which in presence of catalyst undergo dehydration reaction to form aromatic HC. Previous study has also reported that total carbon yield from catalytic pyrolysis of torrefied lignin using H^+ZSM-5 at 600 ^{o}C was 1.15 times higher than non-torrefied lignin [10].

Degradation of cellulose as higher torrefaction severity was accompanied by recondensation reactions leading to increase in aromatic components in biomass. Aomatic HC yield was plotted against the aromatic components in biomass and inverse relationship was observed as shown in Figure 3.11 (b). This shows that the secondary pyrolysis of such recondensed structure does not favor aromatic HC production from catalytic pyrolysis. Repolymerization and secondary pyrolysis of levoglucosan has already been proven to be important pathway for formation of char [47-49]. As a result, the yield of light weight oxygenates can decrease, thus reducing the yield of aromatic HC during catalytic pyrolysis. Significant decrease in aromatic HC yield and total carbon yield from sample torrefied at 275^{o}C-45min is due to severe charring of the sample as a

result complete decomposition of hemicellulose and cellulose.

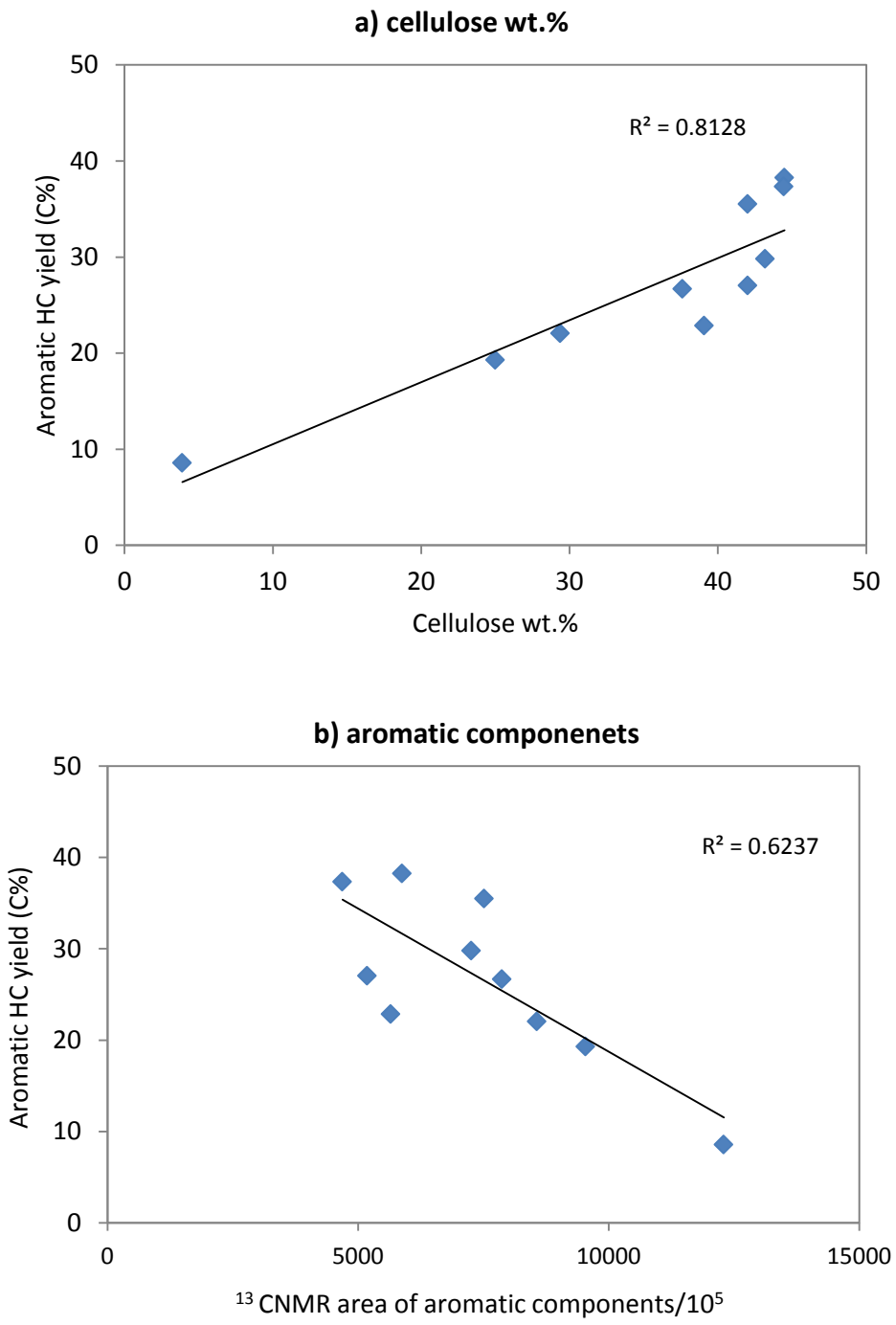

Figure 3.11 Plot of aromatic HC yield from catalytic pyrolysis vs a) wt.% of cellulose and b) aromatic components in biomass

Overall carbon yield accounting for carbon loss during torrefaction:

Aromatic HC production was enhanced by biomass torrefaction in both non-catalytic and H^+ZSM-5 catalyzed fast pyrolysis and phenolic production was enhanced by non-catalytic pyrolysis. However, during calculation of product yield, carbon lost during torrefaction has not been accounted and this increase can just be due to lower O/C ratio in torrefied samples as compared to the control sample. Thus, overall yields were also calculated taking into account carbon lost during torrefaction for both non-catalytic and catalytic pyrolysis. The following equation (Eq. 7) was used to calculate the overall yield accounting for carbon/mass loss during torrefaction.

$$\%\ carbon\ yield = \frac{mass\ of\ compound\ \times mass\ fraction\ of\ carbon\ in\ each\ compound}{mass\ of\ biomass\ before\ torrefaction\ \times mass\ fraction\ of\ carbon\ in\ control\ sample} \times 100$$

(Eq.7)

The results from the overall carbon yield are shown in Table 3.11. It was found that aromatic HC yield from the torrefied samples (275^{o}C-30min for non-catalytic and 225^{o}C-30min and 250^{o}C-15min for catalytic) were still significantly higher than that from raw samples. Also the increase in overall phenolic yield from non-catalytic pyrolysis from torrefied samples 225^{o}C-30min to 275^{o}C-45min was significant as shown in Table 3.11. Thus, increase in yield cannot just be attributed to higher carbon % in torrefied biomass. A number of factors including changes in lignin structure, degradation of hemicellulose and catalyst properties are all responsible for increase in aromatic HC yield from torrefied biomass.

Table 3.11 Product yield from catalytic and non-catalytic pyrolysis accounting for carbon loss during torrefaction

Sample	Non-catalytic pyrolysis (C%)			Catalytic pyrolysis (C%)	
	Aromatic yield	Phenolic yield	Total carbon yield	Aromatic yield	Total carbon yield
Control	0.13^{b}	0.99^{c}	$6.78^{a,b}$	$22.86^{c,d,e}$	$23.06^{b,c,d}$
225°C-15min	0.13^{b}	$1.41^{b,c}$	$6.71^{a,b}$	$26.43^{a,b,c,d}$	$26.76^{a,b,c}$
225°C-30min	$0.14^{a,b}$	2.45^{a}	$7.36^{a,b}$	$35.08^{a,b}$	35.53^{a}
225°C-45min	$0.16^{a,b}$	$2.29^{a,b}$	$5.33^{a,b}$	$23.30^{b,c,d,e}$	$23.67^{a,b,c,d}$
250°C-15min	$0.17^{a,b}$	2.59^{a}	8.38^{a}	35.27^{a}	35.96^{a}
250°C-30min	$0.16^{a,b}$	2.54^{a}	$6.50^{a,b}$	$28.90^{a,b,c}$	$29.61^{a,b}$
250°C-45min	$0.15^{a,b}$	2.43^{a}	$5.44^{a,b,c}$	$16.51^{d,e,f}$	$16.66^{c,d,e}$
275°C-15min	$0.16^{a,b}$	2.72^{a}	$8.25^{a,b}$	$24.71^{a,b,c,d,e}$	$25.08^{a,b,c,d}$
275°C-30min	0.24^{a}	2.58^{a}	$5.41^{a,b,c}$	$14.21^{e,f}$	$14.41^{d,e}$
275°C-45min	0.21^{b}	$1.94^{a,b}$	2.76^{c}	5.47^{f}	5.50^{e}

Any two means in the same column with different letters are significantly different ($p<0.05$) by the Tukey's HSD test. The letters a-f in superscript refer to the highest estimates to the least.

3.6. Conclusions

Effects of torrefaction temperature and residence time on biomass structure and subsequently on the product distribution from non-catalytic and H^{+}ZSM-5 catalyzed fast pyrolysis were investigated. Aromatic HC yield of 38% was obtained from catalytic fast pyrolysis of pine wood torrefied at 225°C-30min, which was 67% higher than catalytic pyrolysis of raw pine. At this torrefaction condition, cellulose degradation had not started; degradation of hemicellulose was 29.6 wt. % and de-etherification and de-methoxylation of lignin were 53% and 35.4% respectively. Torrefaction pretreatment is a crucial step in catalytic pyrolysis of lignocellulosic biomass that can increase aromatic HC yield. However, torrefaction process parameters: temperature and residence time; should be properly adjusted in order to maximize the yield. The

results from this study suggest that the optimum torrefaction condition for catalytic pyrolysis should allow significant degradation of hemicellulose and de-etherification and de-methoxylation of lignin, without causing any loss of cellulose.

3.7. References

1. Bridgwater, A. and G. Peacocke, *Fast pyrolysis processes for biomass.* Renewable and Sustainable Energy Reviews, 2000. **4**(1): p. 1-73.

2. Czernik, S. and A. Bridgwater, *Overview of applications of biomass fast pyrolysis oil.* Energy & Fuels, 2004. **18**(2): p. 590-598.

3. Oasmaa, A. and S. Czernik, *Fuel oil quality of biomass pyrolysis oils state of the art for the end users.* Energy & Fuels, 1999. **13**(4): p. 914-921.

4. Boateng, A.A. and C.A. Mullen, *Fast pyrolysis of biomass thermally pretreated by torrefaction.* Journal of Analytical and Applied Pyrolysis, 2013. **100**(0): p. 95-102.

5. Srinivasan, V., et al., *Catalytic pyrolysis of torrefied biomass for hydrocarbons production.* Energy & Fuels, 2012. **26**(12): p. 7347-7353.

6. Liaw, S.-S., et al., *Effect of pretreatment temperature on the yield and properties of bio-oils obtained from the auger pyrolysis of Douglas fir wood.* Fuel, 2013. **103**: p. 672-682.

7. Meng, J., et al., *The effect of torrefaction on the chemistry of fast-pyrolysis bio-oil.* Bioresource Technology, 2012. **111**(0): p. 439-446.

8. Zheng, A., et al., *Effect of torrefaction temperature on product distribution from two-staged pyrolysis of biomass.* Energy & Fuels, 2012. **26**(5): p. 2968-2974.

9. Ren, S., et al., *The effects of torrefaction on compositions of bio-oil and syngas from biomass pyrolysis by microwave heating.* Bioresource Technology, 2013. **135**: p. 659-664.

10. Adhikari, S., V. Srinivasan, and O. Fasina, *Catalytic pyrolysis of raw and thermally treated lignin using different acidic zeolites.* Energy & Fuels, 2014. **28**(7): p. 4532–4538.

11. Srinivasan, V., et al., *Catalytic pyrolysis of raw and thermally treated cellulose using different acidic zeolites.* BioEnergy Research, 2014. **7**(3): p. 867-875.

12. Zheng, A., et al., *Catalytic fast pyrolysis of biomass pretreated by torrefaction with varying severity.* Energy & Fuels, 2014. **28**(9): p. 5804-5811.

13. Carter, C., et al., *Physicochemical properties of thermally treated biomass and energy requirement for torrefaction.* Transactions of the ASABE, 2013. **56**(3): p. 1093-1100.

14. Tumuluru, J.S., et al., *Biomass torrefaction process review and moving bed torrefaction system model development*. 2010, Idaho National Laboratory (INL).

15. Wen, J.-L., et al., *Understanding the chemical and structural transformations of lignin macromolecule during torrefaction.* Applied Energy, 2014. **121**: p. 1-9.

16. Ben, H. and A.J. Ragauskas, *Torrefaction of Loblolly pine.* Green Chemistry, 2012. **14**(1): p. 72-76.

17. Melkior, T., et al., *NMR analysis of the transformation of wood constituents by torrefaction.* Fuel, 2012. **92**(1): p. 271-280.

18. Hill, S.J., W.J. Grigsby, and P.W. Hall, *Chemical and cellulose crystallite changes in< i> Pinus radiata</i> during torrefaction.* Biomass and Bioenergy, 2013. **56**: p. 92-98.

19. Cabiac, A., et al., *Cellulose reactivity and glycosidic bond cleavage in aqueous phase by catalytic and non catalytic transformations.* Applied Catalysis A: General, 2011. **402**(1–2): p. 1-10.

20. Yang, H., et al., *Characteristics of hemicellulose, cellulose and lignin pyrolysis.* Fuel, 2007. **86**(12–13): p. 1781-1788.

21. Di Blasi, C. and M. Lanzetta, *Intrinsic kinetics of isothermal xylan degradation in inert atmosphere.* Journal of Analytical and Applied Pyrolysis, 1997. **40**: p. 287-303.

22. Glasser, W.G., R.A. Northey, and T.P. Schultz, *Lignin: historical, biological, and materials perspectives*. 2000: American Chemical Society Washington, DC.

23. Mohan, D., C.U. Pittman, and P.H. Steele, *Pyrolysis of Wood/Biomass for Bio-oil: A Critical Review.* Energy & Fuels, 2006. **20**(3): p. 848-889.

24. Adler, E., *Lignin chemistry—past, present and future.* Wood Science and Technology, 1977. **11**(3): p. 169-218.

25. Sharma, R.K., et al., *Characterization of chars from pyrolysis of lignin.* Fuel, 2004. **83**(11): p. 1469-1482.

26. Carlson, T.R., et al., *Catalytic fast pyrolysis of glucose with HZSM-5: the combined homogeneous and heterogeneous reactions.* Journal of Catalysis, 2010. **270**(1): p. 110-124.

27. Sluiter, A., et al., *Determination of structural carbohydrates and lignin in biomass.* Laboratory Analytical Procedure, National Renewable Energy Laboratory, 2008.

28. Segal, L., et al., *An empirical method for estimating the degree of crystallinity of native cellulose using the x-ray diffractometer*. Tex Res J, 1962. **29:786-794**(29): p. 786-794.

29. Thangalazhy-Gopakumar, S., et al., *Production of hydrocarbon fuels from biomass using catalytic pyrolysis under helium and hydrogen environments.* Bioresource Technology, 2011. **102**(12): p. 6742-6749.

30. Sannigrahi, P., et al., *Pseudo-lignin and pretreatment chemistry*. Energy & Environmental Science, 2011. **4**(4): p. 1306-1310.

31. Wallace, G., et al., *Extraction of phenolic-carbohydrate complexes from graminaceous cell walls.* Carbohydrate Research, 1995. **272**(1): p. 41-53.

32. Zawadzki, J. and M. Wisniewski, *^{13}C NMR study of cellulose thermal treatment.* Journal of Analytical and Applied Pyrolysis, 2002. **62**(1): p. 111-121.

33. Bardet, M., L. Emsley, and M. Vincendon, *Two-dimensional spin-exchange solid-state NMR studies of ^{13}C-enriched wood.* Solid State Nuclear Magnetic Resonance, 1997. **8**(1): p. 25-32.

34. Ben, H. and A.J. Ragauskas, *NMR characterization of pyrolysis oils from Kraft lignin.* Energy & Fuels, 2011. **25**(5): p. 2322-2332.

35. Britt, P.F., et al., *Flash vacuum pyrolysis of methoxy-substituted lignin model compounds.* The Journal of Organic Chemistry, 2000. **65**(5): p. 1376-1389.

36. Park, S., et al., *Research cellulose crystallinity index: measurement techniques and their impact on interpreting cellulase performance.* Biotechnol Biofuels, 2010. **3**(10).

37. Sannigrahi, P., A. Ragauskas, and S. Miller, *Effects of two-stage dilute acid pretreatment on the structure and composition of lignin and cellulose in loblolly pine.* BioEnergy Research, 2008. **1**(3-4): p. 205-214.

38. Branca, C., et al., *Effects of the torrefaction conditions on the fixed-bed pyrolysis of Norway spruce.* Energy & Fuels, 2014. **28**(9): p. 5882-5891.

39. Yang, Z., et al., *Effects of torrefaction and densification on switchgrass pyrolysis products.* Bioresource Technology, 2014.

40. Zheng, A., et al., *Effect of torrefaction on structure and fast pyrolysis behavior of corncobs.* Bioresource Technology, 2013. **128**(0): p. 370-377.

41. Bai, X., et al., *Formation of phenolic oligomers during fast pyrolysis of lignin.* Fuel, 2014. **128**: p. 170-179.

42. Zheng, A., et al., *Effect of crystal size of ZSM-5 on the aromatic yield and selectivity from catalytic fast pyrolysis of biomass.* Journal of Molecular Catalysis A: Chemical, 2014. **383–384**(0): p. 23-30.

43. Wang, K., K.H. Kim, and R.C. Brown, *Catalytic pyrolysis of individual components of lignocellulosic biomass.* Green Chemistry, 2014. **16**(2): p. 727-735.

44. Carlson, T.R., et al., *Aromatic production from catalytic fast pyrolysis of biomass-derived feedstocks.* Topics in Catalysis, 2009. **52**(3): p. 241-252.

45. Carlson, T.R., et al., *Production of green aromatics and olefins by catalytic fast pyrolysis of wood sawdust.* Energy & Environmental Science, 2011. **4**(1): p. 145-161.

46. Patwardhan, P.R., R.C. Brown, and B.H. Shanks, *Understanding the fast pyrolysis of lignin.* ChemSusChem, 2011. **4**(11): p. 1629-1636.

47. Kawamoto, H., M. Murayama, and S. Saka, *Pyrolysis behavior of levoglucosan as an intermediate in cellulose pyrolysis: polymerization into polysaccharide as a key reaction to carbonized product formation.* Journal of Wood Science, 2003. **49**(5): p. 469-473.

48. Kawamoto, H., W. Hatanaka, and S. Saka, *Thermochemical conversion of cellulose in polar solvent (sulfolane) into levoglucosan and other low molecular-weight substances.* Journal of Analytical and Applied Pyrolysis, 2003. **70**(2): p. 303-313.

49. Liu, C., et al., *Catalytic fast pyrolysis of lignocellulosic biomass.* Chemical Society Reviews, 2014. **43**(22): p. 7594-7623.

4. Summary and Future Recommendations

4.1. Summary

Effects of torrefaction on structure of major constituents of biomass: cellulose, hemicellulose and lignin and how it subsequently affects the product yield from fast pyrolysis were investigated. The optimum torrefaction condition for lignocellulosic biomass to maximize the yield from catalytic fast pyrolysis using H^+ZSM-5 was also determined. From the results of this study, it can be suggested that torrefaction temperature and residence time of biomass should be severe enough to cause degradation of hemicellulose and depolymerization of lignin via de-methoxylation and de-etherification. Cleavage of ether linkages and methoxyl components of lignin led to increased phenolic yield, which can dehydrate to form aromatic HC in presence of catalyst. Removal of hemicellulose at mild torrefaction condition increased the fraction of cellulose in the biomass leading to increased production of aromatic HC. Since fraction of cellulose in biomass is directly proportional to the aromatic HC yield from CFP, the torrefaction temperature and residence time should not be so high that it can cause cellulose decomposition. Also, decomposition of cellulose is accompanied by recondensation, repolymerization and charring which can increase the aromatic structures in biomass. Such aromatic structures in biomass were found to be inversely related to aromatic HC yield during CFP, implying that secondary pyrolysis of such structures does not favor production of aromatic HC during CPF. For loblolly pine used in this study, torrefaction condition of 225^{o}C-30min and 250^{o}C-15min yielded significantly higher aromatic HC and total carbon yield compared to control sample. The

aromatic HC yield from these samples was approx. 38 % and was 67% higher than catalytic pyrolysis of non-torrefied pine. A new insight on torrefaction chemistry and its effects on hydrocarbons yields were developed in this study. This can be useful in controlling the end product distribution from non-catalytic pyrolysis and in determining the optimum torrefaction condition to be used to maximize aromatic hydrocarbon yield from CFP.

4.2. Recommendations

The original fraction of cellulose, hemicellulose and lignin can vary in different biomass types, so the torrefaction temperature and residence time should be properly adjusted according to biomass. Also, structures of these biomass components vary according to types and species. For example, the fraction of hemicellulose is higher in hardwood than in softwood and it also has different structures. The structure of lignin in hardwood and softwood is also different: guaiacyl lignin is more common in softwood while guaiacyl-syringyl lignin is typically found in many hardwoods. Thus, it is recommended that further studies be conducted with other torrefied bio-energy feedstocks like switchgrass and hardwood. Different model lignin compounds containing different types of lignin linkages and in different ratios can also be investigated to gain proper insight in depolymerization and conversion of these linkages during CPF. Bench scale reactors like fluidized bed and fixed bed pyrolysis reactors could be used to get more practical results on larger scale. CFP of lignocellulosic biomass using zeolite catalyst is an important method for production of highly deoxygenated bio-oil in a single step. However, decrease in yield due to catalyst coking of bio-oil has been a major drawback of CFP process. In this study spent catalyst was not analyzed for coke formation and it is recommended in future analyses using torrefied

biomass. Better estimates for torrefaction temperature and residence times can then be made for optimum conversion of different types of biomass using CFP process.

APPENDIX A: Component and ^{13}C NMR analyses

Table A.1 Results of component analysis, wt.%, dry basis (Not normalized by mass loss)

Sample	Cellulose % (Glucan)	Hemicellulose %					Lignin %		Extractives %
		Xylan	Galactan	Arabinan	Mannan	Total	AIL	ASL	
Control	39.08	6.88	2.94	1.87	12.51	24.21	30.29	1.00	2.99
225°C-15min	42.01	8.01	2.86	1.25	13.79	25.91	30.10	0.98	2.53
225°C-30min	44.49	5.26	1.78	0.60	11.44	19.08	25.99	0.98	3.48
225°C-45min	37.61	1.73	0.26	0.00	5.26	7.25	51.60	0.99	2.60
250°C-15min	44.45	5.96	1.96	0.72	12.15	20.79	30.07	0.95	3.21
250°C-30min	42.01	1.36	nd	nd	4.88	6.24	47.33	0.90	2.66
250°C-45min	29.38	0.41	nd	nd	1.94	2.35	66.93	0.82	1.93
275°C-15min	43.19	3.15	0.53	0.26	7.35	11.29	50.25	0.89	2.09
275°C-30min	24.99	nd	nd	nd	nd	nd	75.33	0.75	1.81
275°C-45min	3.89	nd	nd	nd	nd	nd	99.64	0.26	0.90

Cellulose, hemicellulose and lignin are in extractive free basis
nd: not detected

Table A.2 ^{13}C NMR Area (Not normalized by mass loss)

Sample	Acetyl Carboxyl	Acetyl Methyl	Glycosidic	Ether linkage	Non-ether Linkage	Lignin Methoxly	Aromatic	Aliphatic
Control	6.97E+07	6.60E+07	3.75E+09	2.31E+08	1.53E+08	3.13E+08	5.65E+08	2.12E+08
225°C-15min	3.47E+07	4.90E+07	3.88E+09	2.04E+08	1.31E+08	2.65E+08	5.18E+08	1.73E+08
225°C-30min	3.65E+07	5.89E+07	2.89E+09	1.20E+08	2.26E+08	2.24E+08	5.88E+08	2.20E+08
225°C-45min	2.81E+07	5.15E+07	2.36E+09	9.76E+07	3.18E+08	2.03E+08	7.87E+08	3.22E+08
250°C-15min	3.72E+07	3.50E+07	2.72E+09	1.78E+08	1.34E+08	1.79E+08	4.69E+08	9.92E+07
250°C-30min	3.65E+07	3.65E+07	2.25E+09	1.30E+08	3.87E+08	2.21E+08	7.52E+08	3.61E+08
250°C-45min	3.05E+07	2.16E+07	1.73E+09	1.03E+08	3.96E+08	2.05E+08	8.57E+08	3.24E+08
275°C-15min	3.41E+07	3.27E+07	2.68E+09	1.90E+08	2.76E+08	2.18E+08	7.26E+08	2.64E+08
275°C-30min	2.73E+07	0.00E+00	1.43E+09	1.18E+08	4.09E+08	2.20E+08	9.54E+08	4.22E+08
275°C-45min	0.00E+00	0.00E+00	5.94E+08	1.23E+08	4.74E+08	1.96E+08	1.23E+09	4.26E+08

APPENDIX B: Data for graphs

Table B.1 ^{13}C NMR normalized area (Data for Figures 3.2 – 3.5)

Sample	Acetyl Carboxyl	Acetyl Methyl	Glycosidic	Ether linkage	Non-ether Linkage	Lignin Methoxly	Aromatic	Aliphatic
Control	4.51E+05	4.27E+05	2.43E+07	1.49E+06	9.92E+05	2.03E+06	3.65E+06	1.37E+06
225°C-15min	2.39E+05	3.38E+05	2.67E+07	1.41E+06	9.02E+05	1.82E+06	3.57E+06	1.19E+06
225°C-30min	2.13E+05	3.44E+05	1.69E+07	7.01E+05	1.32E+06	1.31E+06	3.43E+06	1.28E+06
225°C-45min	1.69E+05	3.10E+05	1.43E+07	5.88E+05	1.92E+06	1.22E+06	4.74E+06	1.94E+06
250°C-15min	2.27E+05	2.14E+05	1.66E+07	1.09E+06	8.19E+05	1.09E+06	2.86E+06	6.05E+05
250°C-30min	2.14E+05	2.14E+05	1.32E+07	7.59E+05	2.27E+06	1.30E+06	4.41E+06	2.12E+06
250°C-45min	1.83E+05	1.29E+05	1.04E+07	6.15E+05	2.38E+06	1.23E+06	5.14E+06	1.94E+06
275°C-15min	2.11E+05	2.03E+05	1.66E+07	1.17E+06	1.71E+06	1.35E+06	4.49E+06	1.63E+06
275°C-30min	1.45E+05	0.00E+00	7.62E+06	6.28E+05	2.18E+06	1.17E+06	5.08E+06	2.24E+06
275°C-45min	0.00E+00	0.00E+00	2.68E+06	5.54E+05	2.14E+06	8.83E+05	5.55E+06	1.92E+06

Table B.2 Selectivity of different groups of compounds for non-catalytic pyrolysis (Data for Figure 3.7)

Sample	Selectivity %				
	Aromatics	Furans	Phenolic	Guaiacols	Ketones
Control	1.93	45.25	14.63	34.60	3.59
225°C-15min	1.95	42.07	20.99	28.48	6.51
225°C-30min	1.96	29.87	33.29	30.74	4.14
225°C-45min	3.05	26.49	42.92	24.63	2.90
250°C-15min	2.07	31.49	30.87	31.70	3.88
250°C-30min	2.39	24.01	39.13	31.96	2.51
250°C-45min	2.84	20.81	44.74	28.70	2.90
275°C-15min	1.92	28.95	32.92	35.30	0.91
275°C-30min	4.43	16.01	47.71	31.15	0.70
275°C-45min	7.58	3.38	70.63	17.36	1.06